SENSITIVITY ANALYSIS OF ENERGY PERFORMANCE AND THERMAL COMFORT THROUGHOUT BUILDING DESIGN PROCESS

Richard Gagnon[1], Louis Gosselin[1,*], Stéphanie Decker[2]

[1]Département de génie mécanique, Université Laval, Québec City, Québec, Canada G1V 0A6

[2]Centre de Ressources technologiques Nobatek, 67 Rue de Mirambeau 64600 Anglet, France

Abstract

In a traditional building design process (TDP), design variables are fixed sequentially, as opposed to integrated design process (IDP) which tends to avoid sequential design phases to create more sustainable buildings. First, a reference building is introduced and an energy model based on TRNSYS is presented to determine the energy consumption and comfort in the building. The model is validated based on energy bills, certified simulations and literature. Then, the paper performs an extended sensitivity analysis (SA) of 30 design variables with respect to different performance criteria related to energy consumption and comfort, based on a TRNSYS model. Three SA techniques were used, namely standard regression coefficients (SRC), partial rank correlation coefficients (PRCC) and Sobol indices. Results show that all three techniques yielded a similar ranking of the importance of the variables for most model outputs. Interactions between variables were identified with second-order Sobol indices. In the second part of this paper, a traditional design framework was adopted in which sets of variables were fixed sequentially. A SA was performed at each phase of the process, assuming fixed values for parameters chosen in previous design phases. Results show that fixing variables during the phases of a traditional design process tends to reduce the probabilities of finding low-energy consumption designs. Moreover, the influence of some variables was found to change during the design phases.

Keywords: sensitivity analysis; energy consumption; integrated design; thermal comfort; variables interactions.

---

* Corresponding Author: Louis.Gosselin@gmc.ulaval.ca; Tel.: +1-418-656-7829; Fax: +1-418-656-5343.

Nomenclature

C_{ins}	conductivity of insulation material [W/m-K]
$\overline{C_s}$	average positive surface pressure coefficient [-]
Clo	clothing factor [clo]
COP_C	COP of cooling system [-]
COP_H	COP of heating system [-]
D_{oh}	depth of solar overhang [m]
E	annual energy consumption [kWh/m^2]
E_s	sensible heat transfer effectiveness [-]
E_z	air distribution effectiveness [-]
I_{75Pa}	infiltration rate at 75 Pa [m^3/h-m^2]
$\overline{I_p}$	real time leakage rate [ACH]
k	number of variables [-]
L	length of building [m]
Met	metabolic rate [met]
P	power [kW]
$\overline{P}$	average surface pressure [Pa]
PMV	predicted mean vote [-]
PMV_-	number of discomfort hour when it is too cold [hr]
PMV_+	number of discomfort hour when it is too hot [hr]
RH_{sp}	relative humidity set point [%]
S_a	façade surface area [m^2]
S_i	first-order Sobol indice of a specific variables [-]
S_{ij}	second-order Sobol indices [-]
SHGC	solar heat gain coefficient [-]
t	time of the year [min]
T_{out_6}	outside temperature at 6am [˚C]
T_{ins}	thickness of insulation material [m]
T_{flr}	thickness of concrete on top of the CLT floor [m]
T_{sc}	supply air temperature for cooling [°C]
T_{sh}	supply air temperature for heating [°C]
T_{spc}	set point temperature for cooling [°C]
T_{sph}	set point temperature for heating [°C]
U_H	wind speed at the building height [m/s]
U_w	overall windows conductivity [W/m^2-K]
V_a	volume of the zone with infiltration [m^3]
WWR	windows to wall ratio, [%]
y	sum of the β coefficient [-]

Greek letters

β	standard regression coefficient value [-]
Δt	simulation time step [min]
θ	orientation of the building [°]
ν_a	air speed [m/s]
ρ	air density [kg/m^3]
ρc_p	volumetric heat capacity of insulation material [kJ/m^3-k]
σ	standard deviation value of the sample [kWh/m^2 or hr]

Subscripts

CC	cooling coil
E	east
fan	fan
HC	heating coil
HR	heat recovery unit
hum	humidifier
max	maximum
N	north
S	south
tot	total
W	west

Acronyms

ACH	air change per hour
CLT	Cross laminated timber
EA	exhaust air
IDP	integrated design process
OA	outdoor air
PRCC	partial rank correlation coefficient
SA	sensitivity analysis
SRC	standard regression coefficient
TDP	traditional design process
VAV	variable air volume

1 Introduction

The building sector in Canada is responsible for more than 16% of the green gas emissions and 30% of the energy consumption [1], [2]. Worldwide, this sector is even more impactful representing 30% of the green gas emissions and 40% of the energy consumption. Improving building performance can play a crucial role to cope with climate changes and

resources depletion [3]. However, a building being a complex system, the selected design process may be an obstacle for reaching optimized and high performance designs as in certifications such as LEED platinum, Net-Zero or Passive House [4]–[6]. The design and construction of a building require a multidisciplinary team composed of architects, mechanical, electrical, structural and piping engineers, lighting and control specialists, contractors, and so on. Interactions are required between these stakeholders in the design process, but depending on the type of project (e.g., traditional, design build, integrated design, etc.) these interactions can be quite different [7]. Recent studies have highlighted the correlation between the level of interaction in a building design process and the success of a project in term of energy efficiency, cost, comfort and environmental impact [8]–[10]. They all concluded that the more the team is integrated, the more the project is likely to be successful on those aspects. Nevertheless, there are many obstacles limiting the systematic adoption of a more integrated design process.

In addition to the interactions between stakeholders, it is mandatory to consider the interactions between all the design variables and to determine the importance of these variables on the building performance in order to achieve a successful design process. Sensitivity analysis (SA) plays a key role to develop a better understanding of these issues as it aims at finding how a performance is affected by the design variables or their interactions. Garcia has combined first and second-order sensitivity analysis to highlight the interactions between the design variables of an apartment building [11]. He studied the effect of these variables on the yearly energy consumption, the peak power of the heating demand and the summer comfort. Most of the analysis was perform on a single zone model. Heiselberg et al. used several sensitivity analysis techniques to identify the most important variables on building performance. They claimed that when performed in the early stage of a design process, SA helps designers to focus on the significant variables to develop optimized and sustainable buildings [12]. Yu had performed a sensitivity analysis on a building to find the impact of eight design variables on the yearly energy building consumption [13]. It has been found that when the windows to wall ratio was fixed to 25% versus 50%, the most impactful variables were taking different values. As an example, the heat transfer coefficient of the wall affects the variance of the output with a weight of about 30% in the first case and only 15% in the second case. Eisenhower used a derivative-based

approach to perform a SA over 1009 parameters [14]. Some of these parameters concern schedules, materials properties, windows, lights, variable air volume (VAV) fans, outdoor air control, chillers and others. He used the results in order to reduce the number of variables integrated to an optimization process. Another approach is to use a self-adaptive optimization method to reduce the computation time without neglecting important variables [15]. In an early stage, the algorithm uses a simplified building model and later in the process, merges to a more complex tool in order to obtain accurate results.

In this study, the objective is to find which variables have the greatest influence on a series of building model outputs or objective functions throughout the different stages of a design process and to detect interactions between them. Section 2 presents the technical and functional program of the reference case, along with the model that was used to assess its energy and thermal comfort performances. The input variables and their range of possible values are listed in Section 3. A discussion on the different SA techniques that were used are described in Section 4 and Section 5 presents the results of the SA applied on all the design variables. Section 6 shows the evolution of the SA when applied during different phases of a building design process.

2 Building description and models

2.1 Functional and technical program

In order to test the methodology developed in this paper, a real reference case was considered. One major advantage of using a real building is the availability of information and documentations. In particular, architectural and HVAC&R blueprints and energy simulations were provided by the team who designed the building and helped to define and validate the TRNSYS model used in this work.

The building is located in Brossard (Quebec, Canada) and received a LEED NC silver certification. It consists in an office building that was built between 2009 and 2010. The gross floor area is 11,120 m^2, with 5 storeys and a building footprint of 2,083 m^2. The height of the ceilings is 3.3 m for every floor and the total height of each floor is 3.8 m. The main structure is made out of concrete, and the envelope consists in a mixture of curtain walls, windows, aluminum sidings and cement panels. The insulation material is

100 mm thick and mainly composed of mineral wool. In this building, the energy for heating and cooling is mainly provided by 28 geothermal wells combined with 2 condensers and 2 evaporators. This main system is used to supply a hot and a cold water loops. The hot water temperature set point is between 18°C and 45°C according to the ambient temperature and that of the cold water loop, between 6°C and 14°C. The hot and cold water loops are connected to the heating and cooling coils in order to control the supply air temperature. The core of the building is supplied with air at a temperature between 12°C and 20°C and the peripheral zones with air temperature as described in Table 1. The temperature set points are gradually modulated between their minimum and maximum values depending on the heating and cooling signals. The heating or the cooling system is on when the zone temperature goes below 22°C or above 23.3°C respectively. The supply of fresh air is controlled according to the occupation schedule and flows through a heat recovery unit. The air handling unit can supply up to 1430 L/s of fresh air per floor [16].

Table 1 : Peripheral zone supply air temperature set point according to outdoor temperature.

Outdoor air temperature [°C]	Air temperature set point	
	Min. [°C]	Max. [°C]
–30	20	40
+30	10	18

During the sensitivity analysis, several of the building design variables will be changed as described below. However, the general features of the functional and technical program have been preserved.

2.2 Building energy model and validation

In this work, energy simulations of the building were performed with TRNSYS. In order to complete the SA, the model was parametrized so that the design variables that will be described below could be changed automatically when performing simulations, according to a uniform distribution. Since each of the five storeys had similar features, it was decided to consider only one storey in the model for the purpose of the present study. The zoning included five zones, i.e. a central core and one peripheral zone per façade. The floor

dimensions are 67.6 m per 29.8 m with peripheral zones having a depth of 4.5 m. The time step of the simulation has been set to 15 minutes. An evaluation of the precision of the model showed that a time step shorter than 15 minutes did not lead to a better precision but increased significantly the simulation time.

2.2.1. Envelope

The envelope includes the fenestration and an opaque section. The composition of the opaque envelope, from the outside to the inside, is made of a fibrocement panel, a layer of mineral wool, a particle board and plasterboard. The thickness of the insulation layer and its thermal properties can be varied in the model. Windows are fixed. The windows to wall ratio (WWR), overall windows conductivity (U_w) and solar heat gain coefficient (SHGC) are 3 other design variables and can be different for each façade.

2.2.2. Internal loads

Schedules were defined in the model for the internal loads (i.e., equipment, lighting and people). During weekdays, occupation is from 8:00AM to 6:00PM and during weekends the building is unoccupied. The sensible and latent loads are representative of a typical office building [17]. The number of person per floor is fixed to 176 which represents a density of about 12 m^2/person and every person is producing a total of 150 W (50% sensible heat) [18]. The lighting and the other loads were determined in accordance with the loads present in the energy simulation used for the LEED certification and supplied by the building simulation specialists. A total of 10 W/m^2 is dissipated by the lighting and 5.3 W/m^2 by the other pieces of equipment.

2.2.3. Outdoor air

The required outdoor air flow rate was first calculated based on ASHRAE 62.1 [19]. The required outdoor air for the breathing zone (one floor) at full occupancy is 1103 L/s. The air intake was modulated based on the occupancy schedule and recirculation is used when required to satisfy the heating/cooling loads. The required outdoor air intake is determined by adjusting this flow rate with the efficiency of the air diffusion system (E_z), a design variable that can typically vary from 0.8 to 1.2. When the building is not occupied, the air intake is turned off [20].

2.2.4. HVAC&R systems

In the reference building, air is supplied by a main duct loop circulating around the floor plan a few meters from the façade. Additionally, fan-coil units are used close to the envelope to provide extra heating and cooling. For the sake of simplicity, this HVAC&R system was modeled as shown by the schematic representation shown in Fig. 1. It includes fans, a heat recovery unit, a heating coil, a humidifier and a cooling coil. With this model, the ventilation system supplies air in the building core and recirculates air in the 4 perimeter zones [21]. Since the goal of the model is to estimate energy consumption and comfort, and not IAQ, this simplified zoning was considered acceptable.

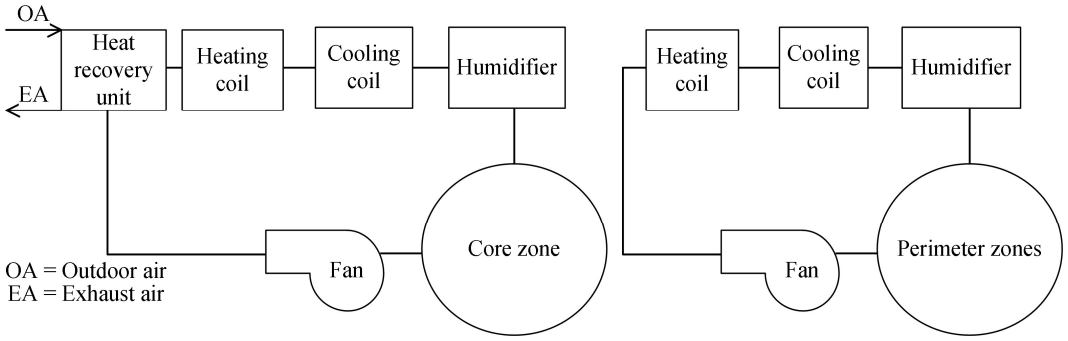

Figure 1 : Schematic representation of the HVAC&R systems.

The temperature in every zone is controlled with a VAV approach, i.e. that the supply air flow varies according to the heating or cooling demand. A proportional controller generates a signal after comparing the zone temperature (T_z) with the cooling and heating set points (T_{spc} and T_{sph}). If $T_{sph} \leq T_z \leq T_{spc}$, the signal is 0 and only the required fresh air is supplied to the core zone. If $T_{sph} - T_z = 1$ or $T_z - T_{spc} = 1$, the signal is 1 and multiplies the maximum air flow defined for each zone. A signal of 0.5 means that 50% of the maximum air flow is supplied to the zone. The power drawn by the fan is approximated by a linear relation with the supply air flow. During the coldest day, the maximum available air flow is sufficient to maintain T_{sph} in each zone. The required power of a centrifugal fan to supply this maximum flow is determined from the table “Fan types and size range” provided in Ref. [22].

The heating and cooling coils have an unlimited capacity (TRNSYS component type 754) in the model in such a way that air temperature can reach the desired supply air temperature set point at all times. The heat transfer rate provided by the heating coil represents the rate

of sensible energy that is added to the air stream. For the cooling coil, it represents the rate of sensible and latent energy removed from the air stream. Finally, the relative humidity is controlled in heating conditions based on a set point in each zone and the model determines the latent energy demand for humidification of this zone. During the summer months (June to September), humidity is not mechanically controlled.

2.3 Model outputs for sensitivity analysis

Based on the model described above, it is possible to calculate several outputs. The annual energy consumption can be calculated by summing the energy consumed by the fans, the heat recovery unit and the energy required for the air conditioning (cooling, heating and humidifying):

$$E_{tot} = \sum_{t=0}^{\frac{60}{\Delta t}\times 8759} ((P_{fan}(t) + P_{HR}(t) + \frac{P_{HC}(t)}{COP_H} + \frac{P_{CC}(t)}{COP_C} + P_{hum}(t))\Delta t \qquad (1)$$

where P(t) represents the power at a given time step and Δt, the duration of the time step. The different power values are provided after the energy simulation. Since PH_C and PC_C are the heating and cooling (thermal) loads of the building, conversion factors (COP_H and COP_C) can be used to determine the actual power needed (electricity, gas, etc.). Note that monthly energy consumptions can also be calculated in the same way. Additionally, the peak power demand P_{max} was also determined from the simulation as it is an important parameter for equipment sizing and in order to establish energy cost:

$$P_{max} = \max((P_{fan}(t) + P_{HR}(t) + \frac{P_{HC}(t)}{COP_H} + \frac{P_{CC}(t)}{COP_C} + P_{hum}(t)) \qquad (2)$$

Thermal comfort can also be assessed by TRNSYS simulations. Calculations are based on ISO 7730 [18], [23] and ASHRAE 55-2004 [24].Based on Fanger's thermal comfort model, the Predicted Mean Vote (PMV) in each zone is obtained. The PMV varies from –3 (very cold) to +3 (very hot) and is influenced by the operative temperature and humidity, but also by clothing factor (Clo), metabolic rate (Met) and air velocity v_a. To determine Clo, the results from [25] have been used. People's behavior and choice of clothes change depending on the outside weather and the following correlation is used:

$$\mathrm{Clo_{mean}} = -0.01 \times \mathrm{T_{out\_6}} + 0.766 \quad (3)$$

where T_{out_6} is the temperature at 6:00AM in °C. Concerning Met and v_a, their values were fixed to 1.2 and 0.15 m/s [24].The evaluation of thermal comfort on a yearly basis is computed via 2 indicators defined as the number of discomfort hour PMV_-, PMV_+ [26]:

$$\mathrm{PMV\_} = \sum_{t=0}^{\frac{60}{\Delta t}8759} (X_t \Delta t) \quad (4)$$

with:

$$X_t = \begin{cases} 1 & \text{if PMV} \leq -0.5 \\ 0 & \text{else} \end{cases} \quad (5)$$

Note that only the occupation hours were considered. PMV_+ is calculated in the same way, except that $X_t = 1$ when PMV ≥ 0.5. According to ASHRAE 55.2004, the acceptable PMV for a general comfort is fulfilled when: –0.5 < PMV < +0.5. Note that the criteria presented in this section can be calculated in each zone or averaged over the entire floor. Then, it will bear the name PMV_{-N} for the PMV_- in the north zone and the name PMV_{-tot} for an average of PMV_- on the entire floor. Finally, PMV_{tot} represents the sum of PMV_{-tot} and PMV_{+tot}.

2.4 Model validation

To verify the accuracy of the present model, a reference case scenario has been elaborated in order to represent the actual building that was introduced in the beginning of Sections 2.1-2.2. All variables of the models have therefore been chosen to be as close as possible to those of this building in the reference case. The results of this TRNSYS model were compared to:

(i) the energy bills of the reference building introduced in Section 2.1;

(ii) the results of a certified simulation that had been done during the elaboration of the reference building using EE4 (EE4 is a program developed by Natural Resources Canada. It uses a compliance checking approach to building energy simulation. It evaluates building designs according to the Model National Energy Code for Buildings (MNECB) 1997 and "Performance Compliance for Buildings" (MNECB/CS, NRC 1999) [27]);

The energy bill shows that the total yearly electricity consumption from October 2013 to September 2014 was 137.5 kWh/m^2. That includes heating, cooling, ventilation, lighting, computers, domestic hot water, plug loads, etc., since electricity was the only source of energy supplied to the building. However, the energy bill did not explicitly separate HVAC&R loads (which are included in the present model) from other types of loads. Based on literature, it was estimated that ~53% of the energy demand is devoted to heating and cooling in typical office buildings in Québec, Canada [28], which represents ~72.9 kWh/m^2 for the reference buildings. This is very close to the value achieved from the TRNSYS simulation, i.e. 78.6 kWh/m^2 (less than 7% difference).

Figure 2 compares the energy required for heating and cooling the building for each month, with the TRNSYS model and from the certified simulation. The energy intensity for cooling and heating calculated with the TRNSYS model is 78.6 kWh/m^2 compared to 90.6 kWh/m^2 for the EE4 energy simulation. Considering the 13% difference, the results of the present model were considered to be adequate given its relative simplicity. For example, only one floor is included in our model in such a way that thermal losses through the foundations and roof are not taken into account. Furthermore, the zoning includes only five zones, whereas the EE4 simulation includes approximately 30 detailed zones per floor.

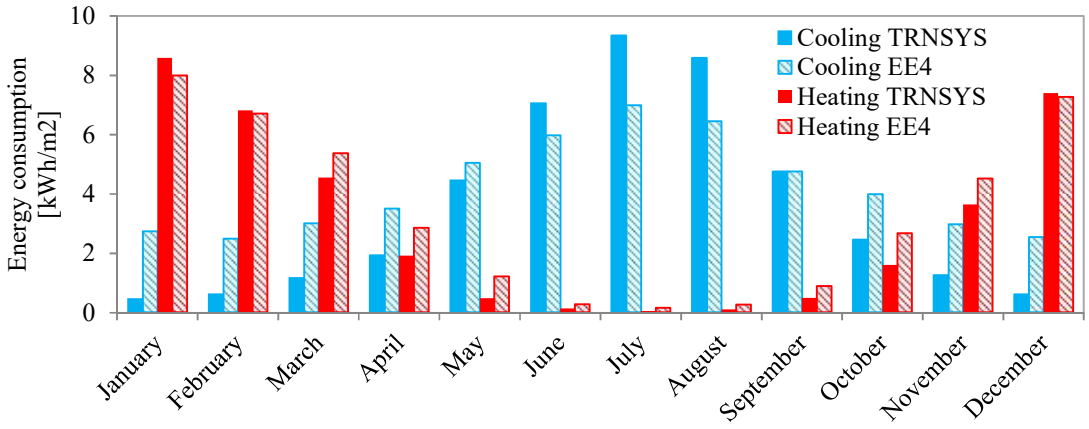

Figure 2: Comparison of the monthly energy consumption for heating and cooling in kWh/m^2 as calculated by the present model and a certified simulation.

Finally, it was verified that the energy intensity for heating and cooling that were calculated by our model were representative of typical values measured in LEED silver buildings. In [29], the average whole-building energy usage of LEED NC buildings in North America

is 195.5 kWh/m^2. Over 35% of the studied buildings where in ASHRAE weather zone 4 (mixed) and 35% in ASHRAE weather zone 5 (cool). Considering that 53% of the energy is used for heating and cooling in Quebec, Canada [28], this means that the LEED NC buildings consume approximately 100 kWh/m^2.

In the end, the present model was thus considered adequate and sufficiently representative of real buildings to perform the sensitivity analysis. Again, it should be emphasized that the objective of the model is not to reproduce exactly a specific building design, but rather to be used for the purpose of the sensitivity analysis.

3 List of input variables and ranges for SA

In the model described above, it was possible to modify different design variables and to determine their impact on energy consumption and thermal comfort. In order to create this list of variables, the work of [26], [30]–[39] has been reviewed to identify inputs that were tested in previous studies. The variables cover different aspects of a building design process. The list of the 30 design variables considered in this study are presented in the next table:

Table 2: List of the design variables and the range of values that they can take.

Variable index and symbol	Description	Range	References
1-C_{ins}	Conductivity of insulation material [W/m-K]	[0.018 - 0.1]	[40]
2-ρc_p	Volumetric heat capacity of insulation material [kJ/m^3-k]	[15 - 500]	[40]
3-T_{ins}	Thickness of insulation material [m]	[0.1 - 0.35]	[40]–[42]
4-I_{75Pa}	Infiltration rate [m^3/h-m^2]	[1.5 - 11]	[43], [44]
5-L	Length of the building [m]	[45 - 71]	
6*-WWR	Windows to wall ratio [%]	[0 - 0.5]	[45]
10*-SHGC	Solar heat gain coefficient [-]	[0.2 - 0.7]	[46]
14*-U_w	Overall windows conductivity [W/m^2-K]	[0.8 - 1.6]	[46]
18-θ	Orientation of the building [°]	[0 - 90]	
19-T_{flr}	Thickness of concrete on top of the CLT floor [m]	[0 - 0.25]	
20*-D_{oh}	Depth of solar overhang [m]	[0 - 1.5]	[34], [47]–[49]
24-E_s	Sensible efficiency of heat recovery unit [-]	[0.6 - 0.9]	[50]–[53]
25-T_{sh}	Supply air temperature for heating [°C]	[30 - 40]	[19], [54], [55]
26-T_{sc}	Supply air temperature for cooling [°C]	[12 - 18]	[45], [56]
27-T_{sph}	Set point temperature for heating [°C]	[19 - 23]	[24]
28-T_{spc}	Set point temperature for cooling [°C]	[25 - 27]	[24]
29-RH_{sp}	Relative humidity set point (October to May) [%]	[20 - 50]	[24], [57]
30-E_z	Air distribution effectiveness [-]	[0.8 - 1.2]	[19]

*Note: WWR, SHGC, U_w and D_{oh}, are specified individually for each façade orientation. In other words, they represent a list of 16 variables given for the 4 façades of the building. The index of these design variables increases from north, east, south, and west. As an example, $SHGC_E$ is the 11th variables.

In order to determine a proper range of real infiltration rates, the results of Emmerich and Persily and from ASHRAE handbooks were used [44], [58] combined with the work of Gowri et al. [43]. In the first article, 228 commercial buildings in the USA built between 1960 and 2005 have been studied, all from the NIST database. For every building, the database shows a value of the air leakage expressed in m^3/h per surface area of façade at a pressure difference of 75 Pa. By considering only the five storey buildings in their list, air leakage (I_{75Pa}) ranges from 3.8 to 45 m^3/h-m^2 at 75 Pa. Compared to the typical values in the ASHRAE handbook fundamental (i.e. 1.8 to 11.0 m^3/h-m^2 at 75 Pa), this ranges is quite

large due to the face that the database includes both old and recent buildings (from 1955 to 2005). Since in this paper, we are mostly interested by high performing modern buildings, the second range was chosen.

In this work, the transient infiltration rate in real conditions is determined by following the methodology proposed by Gowri et al. [43]. First, they have determined an average of the positive surface pressure coefficients, namely $\overline{C_s} = 0.617$, which was determined to be applied to all surfaces in the building and this average was found to be weakly influenced by building shape. This coefficient is used to determine an average surface pressure:

$$\overline{P} = 0.5\overline{C_s}\rho {U_H}^2 \tag{6}$$

with $U_{H,}$ the wind speed at the building height and ρ the air density. Then, the real leakage rate expressed in air change per hour (ACH) is found from:

$$\overline{I_p} = I_{75pa}\frac{S_a}{V_a}\left(\frac{\overline{P}}{75}\right)^{0.65} \tag{7}$$

where S_a is the façade surface area and V_a, the volume of zones with infiltration. Every time step, $\overline{I_p}$ is calculated and is included in the energy balance of every peripheral zone.

4 Description of the sensitivity analysis techniques

SA has been applied often in buildings design to explore the influence of variables on several model outputs. Although it can be a powerful tool for designers and building optimization, it is mostly used at an academic level or by sensitivity analysis practitioners in specific domains [59]. There are several methods to perform a sensitivity analysis and each one has specific characteristics. Tian presents a review of SA techniques with their main features [60]. For the purpose of this study, three methods have been used. At first, standard regression coefficients (SRC) β_i are used to sort variables according to their importance (where i gives the position of the variable in Table 2). Matlab 2015 provides a function named “regress”, which was used in this work to get the coefficients. They are suitable for linear models only [61]. Nguyen proposes to select a sample of 1.5 up to 10 times the number of input variables for valid results. The linearity of the model can be assessed by looking at the summation of the square of the β_i coefficient:

$$y = \sum_{i=1}^{k} \beta_i{}^2 \quad (8)$$

The more the summation is close to 1, the more the model is linear and fit [62]. For a non-linear but monotonic model, it is suggested to use another sensitivity analysis technique: partial rank correlation coefficients (PRCC) [61], [63]. With this method, the inputs and the outputs value are sorted in ascending order and their values is replaced by their ranks. From that point, a linear regression model is extrapolated, similarly as for SRC. The detailed methodology is defined in Ref. [64].

The third method used in this paper is suitable for nonlinear and non-monotonic models or for models with strongly correlated inputs and is in the family of SA methods cased on variance decomposition. In this study, the Sobol indices are used. The first-order indices (S_i) measure the effect of a variable i on the output variance. The second order S_{ij} measures the contribution of the interaction between the i^{th} and j^{th} variables on the output variance. For calculating both Sobol indices, the method developed by Plischke has been used [65], In order to determine S_i and S_{ij}, the sample size may vary from hundreds to a few thousands. In this paper, SRC and PRCC are determined from a sample size of 2000, S_i and S_{ij} from a sample size of 10,000. The sample size has been fixed after observing a convergence of each value.

This study first evaluates the linearity of the model outputs with the (SRC) method. If linear, the β_i coefficients are used to perform the SA. If the model is not linear, the second technique (PRCC) is preferred. Finally, Sobol indices are used to detect the interactions between the variables which the first 2 other techniques cannot do.

5 Results from each sensitivity analysis technique

5.1 Evaluation of the model linearity and comparison between SRC and PRCC

As mentioned before, one of the requirements for significant results with this method is to be in presence of a linear system. Table 3 shows the results of Eq. (8) for the principal model outputs assuming $COP_H = COP_C = 1$ for the calculation of E_{tot}. The impact of the COPs values was also investigated in Section 5.2.

Table 3: Evaluation of the model linearity for the main outputs.

	E_{tot}	E_{fan}	E_{hc}	E_{cc}	E_{hum}	PMV_{-N}	PMV_{+N}	PMV_{-W}	PMV_{+W}
y	0.855	0.907	0.967	0.876	0.920	0.608	0.833	0.630	0.842
$\bar{x}$*	77.88	10.34	0.65	54.49	6.32	87.8	1842.0	87.4	1836.6
$\sigma/\bar{x}$	0.138	0.168	0.530	0.160	0.748	1.507	0.208	1.478	0.205
	PMV_{-S}	PMV_{+S}	PMV_{-E}	PMV_{+E}	PMV_{-C}	PMV_{+C}	PMV_{-tot}	PMV_{+tot}	PMV_{tot}
y	0.552	0.807	0.528	0.815	0.831	0.837	0.631	0.855	0.880
$\bar{x}$*	64.0	2068.0	46.7	2180.9	0.7	2670.9	26.82	2414.6	2441.1
$\sigma/\bar{x}$	1.664	0.191	1.659	0.179	0.892	0.0590	1.450	0.078	0.070

* Units for $\bar{x}$ and σ are in kWh/m^2 for E_x and in hr for PMV_x. $\bar{x}$ represents the average of the sample and σ, its standard deviation.

According to Table 3, the model is strongly linear for the different energy criteria, but not so much for comfort indicators. This means that the SRC technique is suitable to rank the importance of the design variables on energy consumption but might not be the best technique for the ranking of the variables to explain the variation of the PMV_+ and PMV_-.

Next, SRC and PRCC results were compared. As mentioned before, PRCC is a valid technique for linear and non-linear monotonic systems.

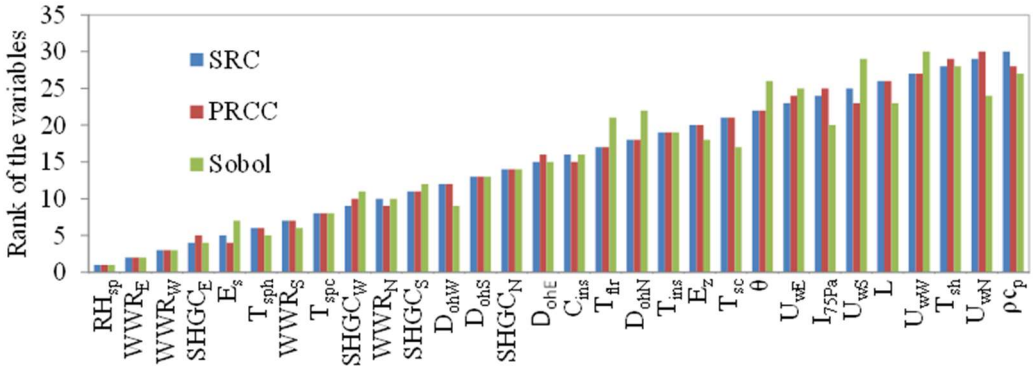

Figure 3 is a comparison of the rank of each variable for E_{tot} using those two techniques. For both techniques, RH_{sp} is the variable that has the largest impact on E_{tot}. This can come from the large range used for the sensitivity analysis for that variable (between 20 and 50%, see Table 2) and the fact that humidification can be an energy intensive process in cold climate due to the low exterior humidity level during winter.

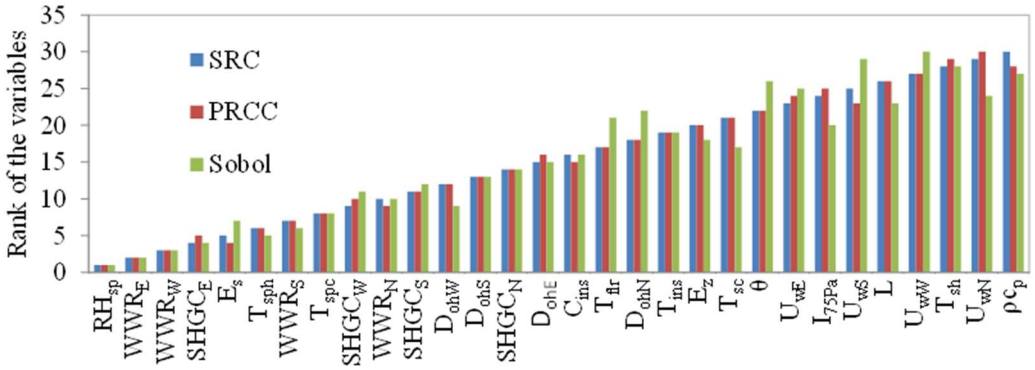

Figure 3: Comparison between the ranked variables with SRC, PRCC and Sobol SA techniques, with respect to E_{tot}.

The same analysis has been performed for the other indicators and in all cases, the two techniques give approximately the same ranking. In the worst case, i.e. for the ranking of PMV_+, $SHGC_S$ was ranked in 9th position with SRC while it was ranked in 12th position for PRCC. Given that the impact of variables at such a rank becomes very weak, this difference is not significant and it can be concluded that both methods give a similar appreciation of the ranking of the variables for all the criteria.

It is also instructive to look at a scatter plot for a visual assessment of the behavior of the model. Figure 4 shows some variables and their impact on selected model outputs.

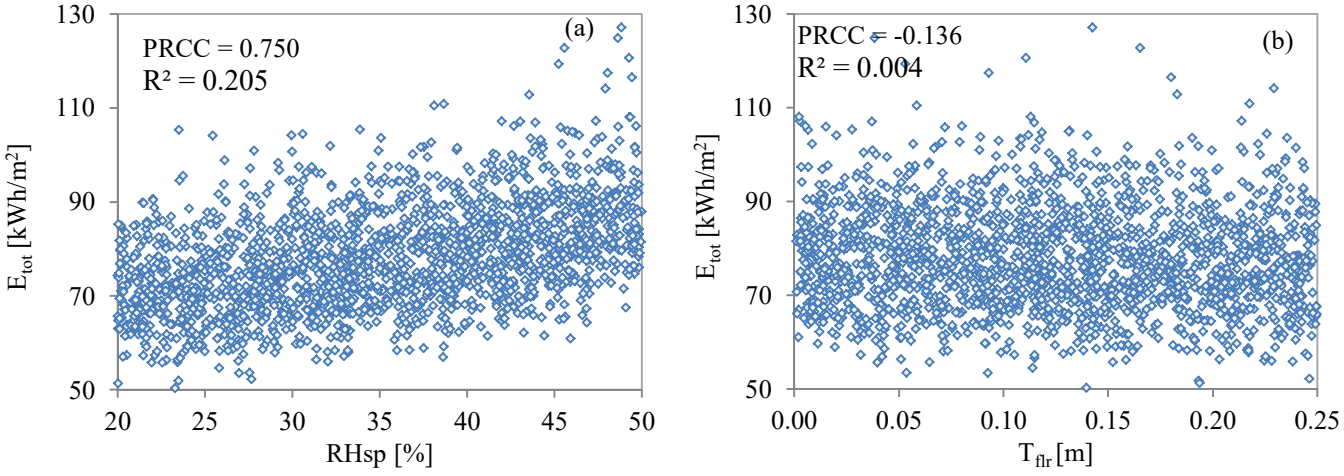

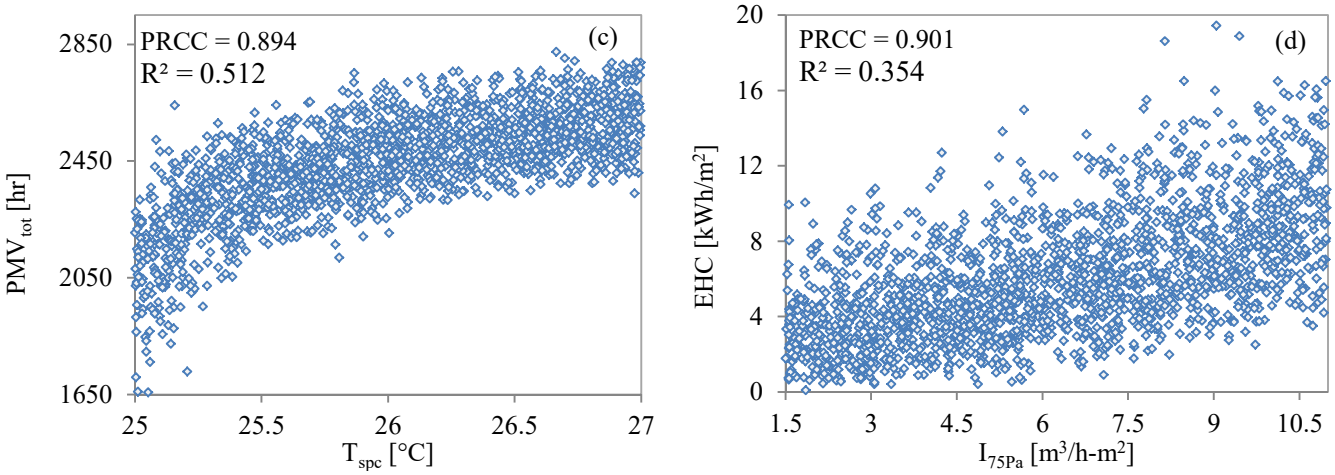

Figure 4: Examples of scatterplots of model outputs as a function of model inputs (a) E_{tot} vs RH_{sp} ($R^2 = 0.20$), (b) E_{tot} vs T_{flr} ($R^2 = 0.004$), (c) PMV_{tot} vs T_{spc} ($R^2 = 0.89$), (d) E_{hc} vs I_{75Pa} ($R^2 = 0.35$).

Figure 4a is an example of a strong linear relationship between RH_{sp} and E_{tot} (PRCC = 0.750) while Fig. 4b represents a weak linear relationship between T_{flr} and E_{tot} (PRCC = -0.136). When the PRCC of a variable has a high value (close to 1), it means that the corresponding variable has a strong influence on the model output. When the coefficients have a small value (PRCC< 0.5), the scatter plot hardly shows any kind of relationship. Figure 4c is an example of a strong monotonic relationship between T_{spc} and PMV_{tot} and finally, Fig. 4d also shows a strong relationship between I_{75pa} and this time, E_{hc}.

Given the analysis presented above, the SA for the energy outputs will be presented using SRC coefficients in Sections 5.2 and 5.3. The comfort function does not behave linearly for all the variables; therefore the SA will be presented using PRCC coefficients in Section 5.4. However, SRC could also have been suitable for that case according to Fig.

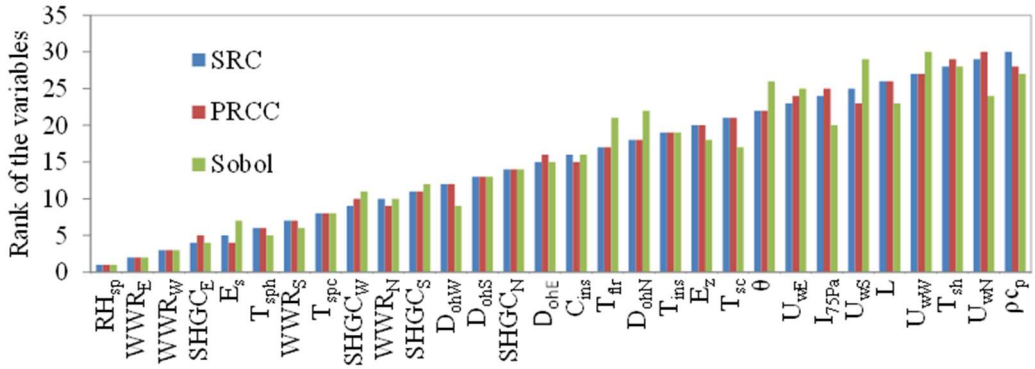

Figure 3.

5.2 Standard regression coefficients for energy outputs

For a better understanding of the results from the SA, the output function E_{tot} was separated into 4 blocks: E_{cc}, E_{hc}, E_{fan} and E_{hum}, i.e. the energy consumption for cooling, heating, ventilating and humidifying respectively. In Fig. 5, the design variables are organized in decreasing order of importance according to the output E_{tot}. The length of each color bar represents the magnitude of β_i. A positive β-value for a given design variable means that increasing that variable leads to an increase of the energy consumption, and vice versa.

Several variables were found to have a significant influence on the total energy consumption. These influential variables include set points (e.g. RH_{sp}, T_{sh} and T_{sc}), windows geometry and properties (WWR, SHGC, D_{oh}), and the efficiency of the heat recovery system (E_s).

Looking at the values of β_i for E_{tot}, one could be tempted to conclude that variables such as C_{ins}, T_{ins} and I_{75Pa} are "irrelevant" parameters since they have low β-values (blue lines in Fig. 5). However, these variables have a significant impact when looking at the annual cooling and heating loads. Some variables, such as the three mentioned above, can increase the energy requirement for cooling, but decrease the energy consumption for heating, or vice versa. In that case, the total energy consumption can appear to be unaffected by that variable, even though the detailed energy budget can be completely different.

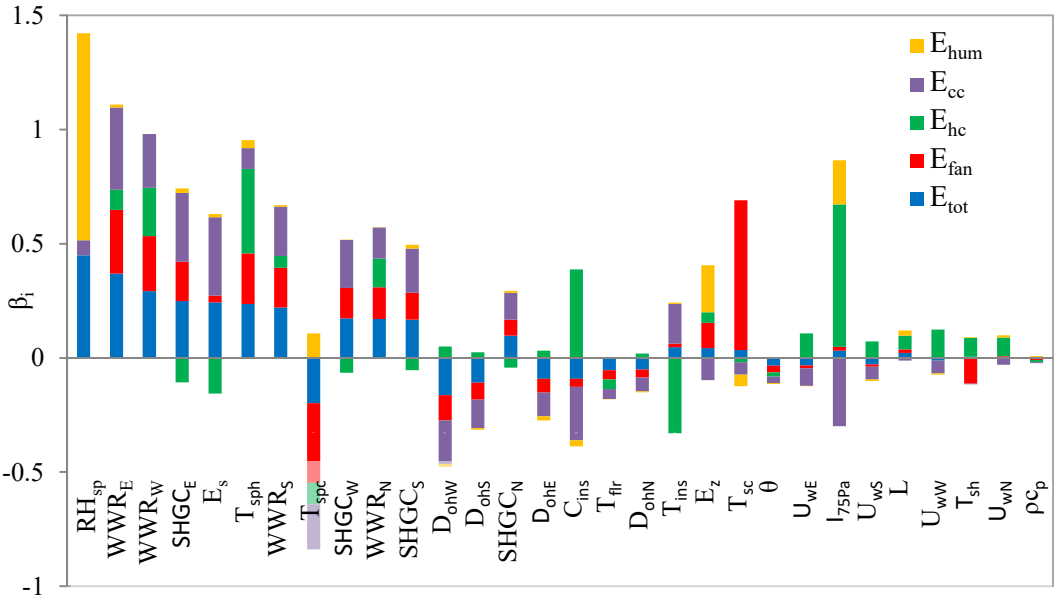

Figure 5: β_i coefficients for each variable and several energy outputs.

Looking at the energy consumption distribution can help to understand which sector will influence the most E_{tot}. As can be seen in Table 3, on average, the energy consumption for cooling has more weight on the total energy consumption than the energy consumption of the heating coil (70% against 8%). However, E_{tot} might not be representative of reality in all the cases, i.e. when COP_C and COP_H is different than one. The weight of the energy for cooling or heating can take different proportions and affect the sensitivity of a given variable. Figure 6 shows the differences between 3 cases with respect to β_i for E_{tot}:

- . $COP_H = COP_C = 1$;
- . $COP_H = 1$ and $COP_C = 3$ (e.g., electrical heating, air-conditioning unit);
- . $COP_H = 4$ and $COP_C = 3$ (e.g., geothermal heating and cooling).

Each variable loses or gains importance depending on the different situations.

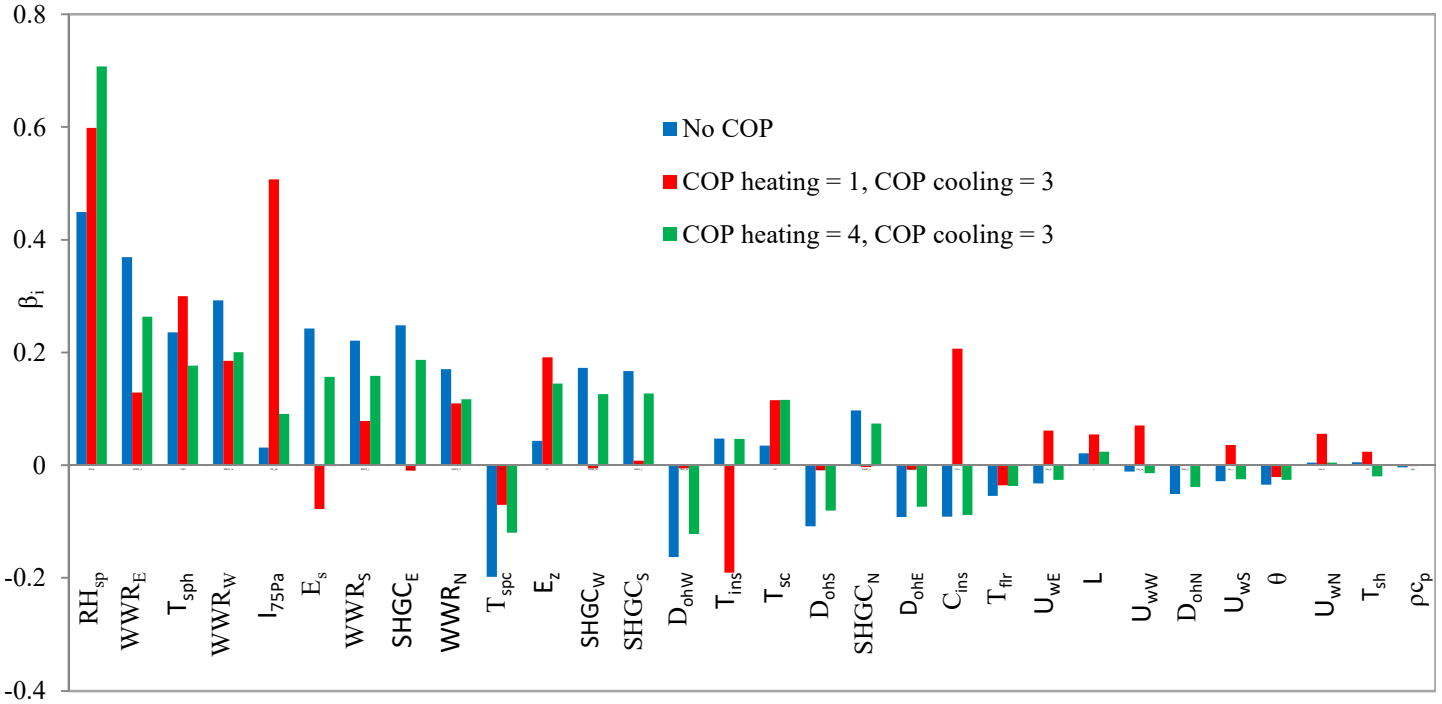

Figure 6: β_i coefficients for each variable when the SA is applied on $E_{tot.}$

For example, I_{75pa} becomes a highly sensitive variable for E_{tot} in the second scenario (red in Fig. 6). The energy saving from infiltrations during warm days are not as important as

in the first scenario with $COP_H = COP_C = 1$. For other variables such as T_{ins} and C_{ins}, the sign of β_i changes according to the situation. Increasing the insulation thickness and the COP_C will reduce the total energy consumption. This indicates that the heating and cooling system characteristics interact with the other parameters and could be considered simultaneously for a robust sensitivity analysis.

Figure 7 shows another representation of the opposition between the variables and their impact on energy consumption. It reports in the same figure the β-values for the heating need (x-axis) and cooling need (y-axis) for each variable.

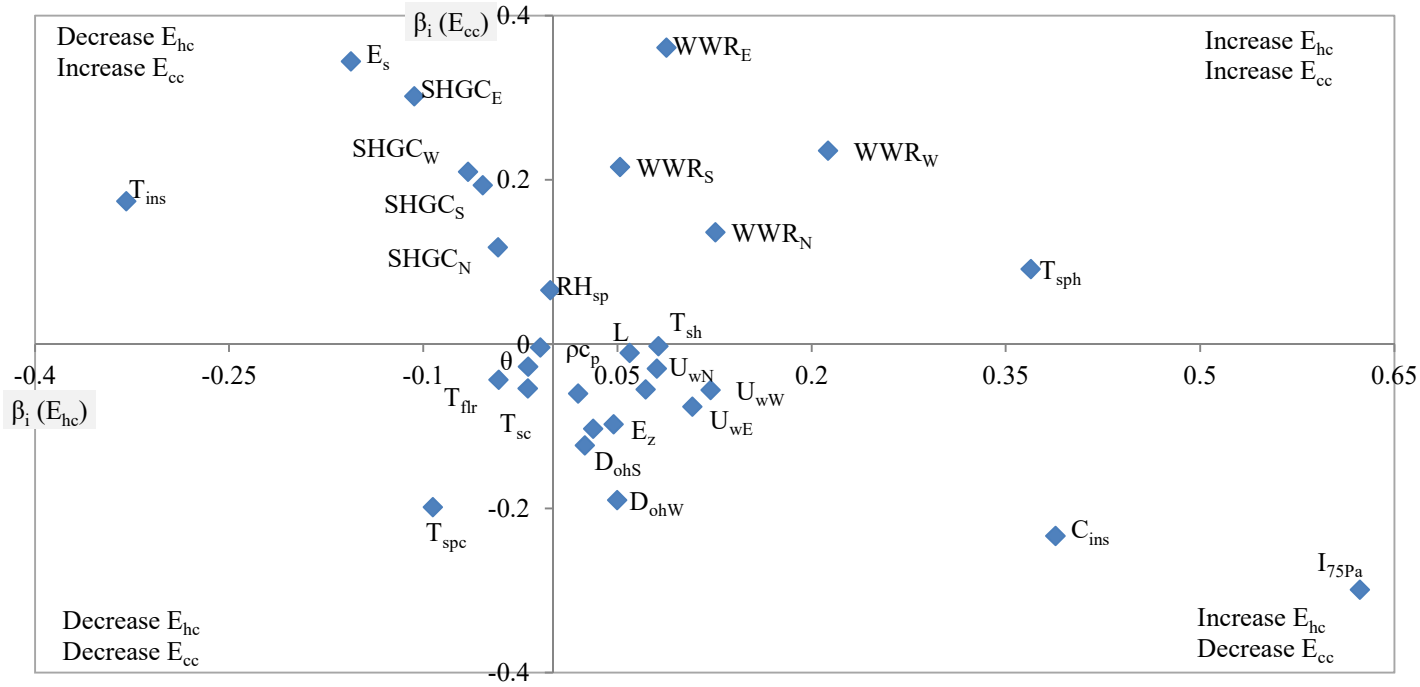

Figure 7: β_i coefficients for each variable when the SA is applied on E_{hc} and E_{cc}.

When a variable is located in the upper right corner, an augmentation of the variable will increase both heating and cooling loads (E_{hc} and E_{cc}). Examples of such variables are the window to wall ratios. The variables in the lower left corner are the ones that when increased lead to a reduction of the energy consumption for both heating and cooling. In this case, those variables are essentially T_{spc}, T_{flr}, T_{sc} and θ. The variables in the upper left and lower right corners tend to increase heating while reducing cooling, or vice versa. The impact of T_{spc} on the heating load can come from the zone-to-zone interactions when different zones are simultaneously requiring heating and cooling.

5.3 Standard regression coefficient for power outputs

An analysis similar to that in Section 5.2 has been applied to the peak power demand (i.e., the maximal instantaneous power demand). In Fig. 8, the design variables are organized in decreasing order of importance according to the output P_{tot}. The variables related to fenestration (WWR, SHGC, D_{oh}) are the ones that have the most influence on P_{tot} and P_{cc}. However, it is not the case for P_{hc}, where the variables related to the opaque envelope are more significant (C_{ins}, T_{ins}). As for E_{tot}, I_{75Pa} is the most important variable with respect to the required power of the heating coil but is not very important for the required power of the cooling coil.

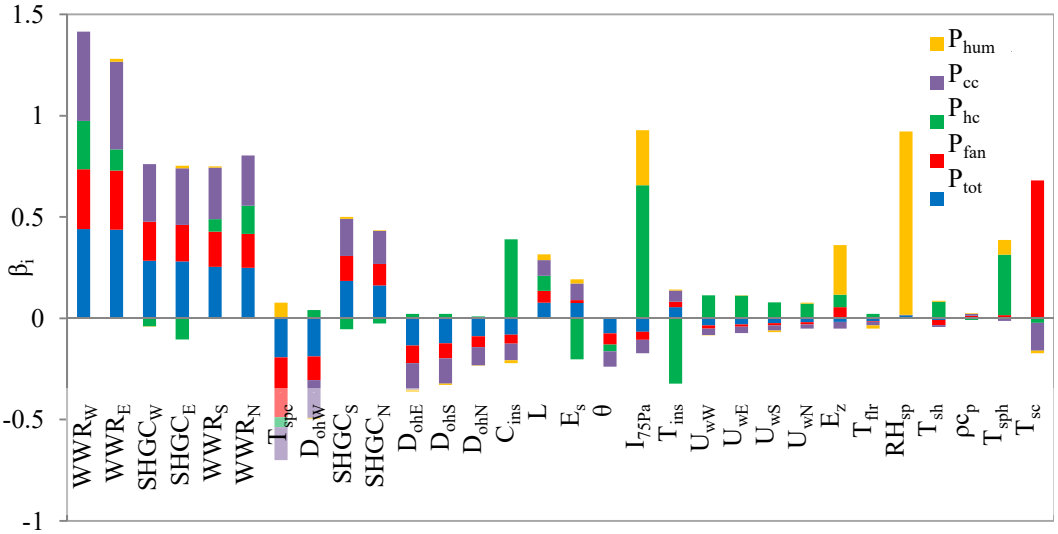

Figure 8: β_i coefficients for each variable and several power model outputs.

In order to compare more effectively whether the different variables impact in a similar manner E_{tot} and P_{tot}, the β-values associated with each variable for these two outputs are reported in Fig. 9. The x-axis provides the β value for E_{tot} and the y-axis, for P_{tot}. As can be seen, most variables have the same impact on E_{tot} and P_{tot}, i.e. their β-values for E_{tot} and P_{tot} are very close.

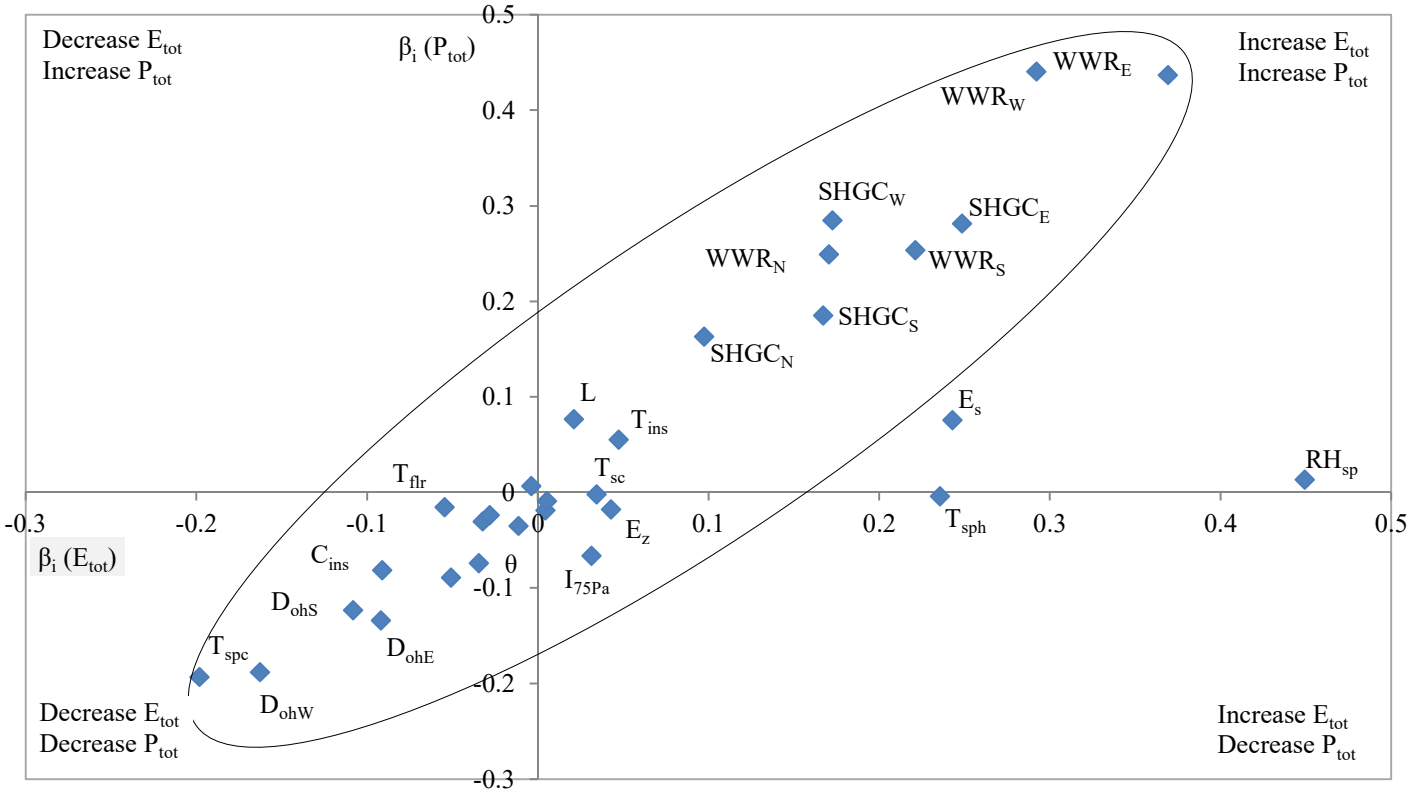

Figure 9 : β_i coefficients for each variable when the SA is applied on E_{tot} and P_{tot}.

It is worth to recall that E_{tot} is closely related to the average of the power demand, but that P_{tot} is the annual peak of the demand. Therefore, the impact of a variable on E_{tot} and on P_{tot} can be quite different. Three variables exhibit a different impact on E_{tot} and P_{tot}. First, increasing the temperature set point (T_{sph}) for heating increased the annual energy consumption. However, it did not affect significantly the maximum required power. When a heating system is turned on in the presence of a higher zone air temperature, it reduces the required heating power to bring this same air to a defined supply zone air temperature (T_{sh}). Second, increasing RH_{sp} will affect E_{tot} but not P_{tot}. To explain this situation, we need to look at the monthly distribution of the observed peak power: 88% of the time, the maximum power is observed between June and September, i.e. when there is no humidification of the air. For that reason, it is normal to see that as RH_{sp} increases, it does not affect the maximum power since most of the time, the maximum power is observed during summer months. Finally, E_s can significantly reduce the total energy consumption without affecting so much the total required power.

5.4 Partial rank correlation coefficients (PRCC) for thermal comfort model outputs

The distributions of PMV_+ and PMV_- among the simulated designs give relevant information that is helpful for the analysis of the PRCCs. They can be observed in Fig. 10, which shows the distribution of PMV_- and PMV_+ in each zone. To plot this figure, the different criteria were calculated for each of the simulated scenarios and the results were grouped into 25 bins. The x-axis represents the number of hours of discomfort and the width of a bin is determined with the following equation:

$$\mathrm{Bin}_{\mathrm{width}} = \frac{\max(\mathrm{PMV}_{+\ \mathrm{or}-\mathrm{in\ zone}}) - \min(\mathrm{PMV}_{+\ \mathrm{or}-\mathrm{in\ zone}})}{25} \quad (9)$$

The y-axis represents the number of observations in each bin.

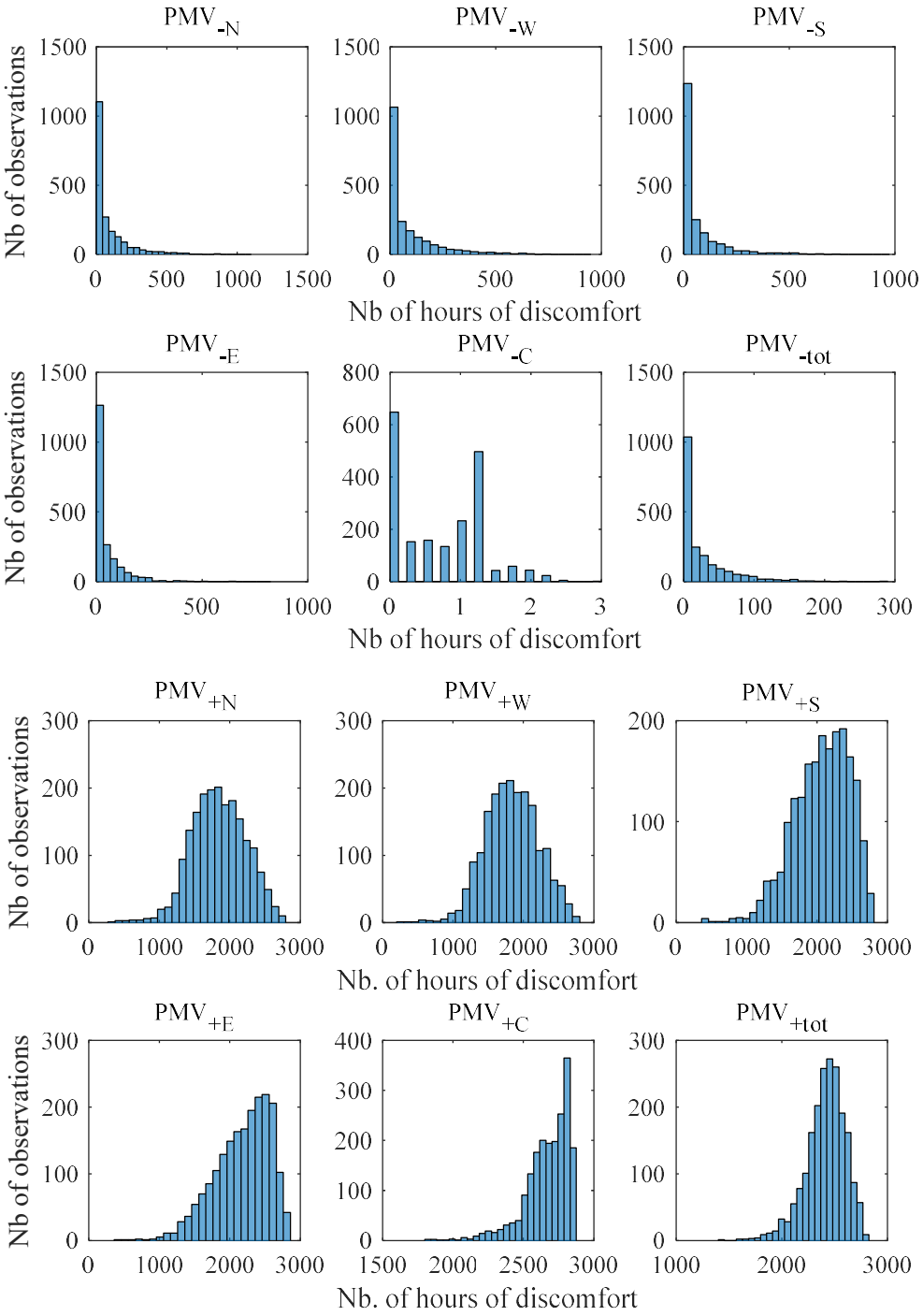

Figure 10: Distribution of the PMV in each zone from the simulation sample.

According to Fig. 10, among all scenarios tested it is rarely too cold (PMV < –0.5) in the different zones as the number of hours for which the comfort criterion is not respected is very small for all cases simulated. On the other hand, the distributions of PMV_+ show that

it is often too hot (PMV > +0.5) in the building in the different scenarios generated during the SA analysis. Comparing results in Fig. 10 with those reported in Table 3, one can see that the PMV criteria for which the most non-linearity was observed are the PMV_{-}. Moreover, the standard deviation divided by the average of the sampling gives another appreciation of the influence of the design variables on PMV_{+} and PMV_{+}. These values are also reported in Table 3 and for PMV_{+} in each zone. Values of standard deviation-to-average of ~1.5 are found for PMV_{+} whereas these values are only around 0.2 for PMV_{-}. In other words, the ranking of the design variables with respect to the PMV_{-} criteria is of little interest since they do not influence these outputs significantly. This can stem from the fact that these criteria were determined using threshold values, as they sum up every hour for which the PMV is above or under +0.5 and –0.5 respectively.

Figure 11 gives a general insight of the most influential variables as it shows the ranking for PMV_{-tot}, PMV_{+tot} and PMV_{tot}. The variables are ranked in order of importance for PMV_{tot}.

Figure 11: PRCC coefficients for each variable and the outputs PMV_{-tot}, PMV_{+tot} and PMV_{tot} for the entire floor.

One of the principal conclusions is that the most important variables for the comfort have an opposite effect on PMV_{-} versus PMV_{+}. It is the case for almost all the variables except T_{flr}, θ, WWR_N and WWR_W. As it is rarely too cold in the zones, PMV_{+tot} dominates PMV_{tot} which means that for all the variables, PMV_{tot} goes in the same direction as PMV_{+tot}. The

temperature set point for cooling and heating are ranked among the most important design variables with the infiltration rate at first. When the value of I_{75Pa} increases, it reduces the situations where it is too hot but increases the number of hours where it is too cold.

Table 4 shows the influence of each design variable in each zone for PMV_+. For a quick overview, the cells are colored from dark red (high negative value) to dark blue (high positive value).

Table 4: PRCC coefficients for each variable with respect to PMV_+ in each zone.

	I_{75Pa}	T_{spc}	C_{ins}	T_{sph}	T_{ins}	θ	RH_{sp}	T_{sc}	$SHGC_E$	WWR_E	$SHGC_S$	$SHGC_N$	$SHGC_W$	E_z	ρc_p
PMV_{+N}	-0.8	0.5	-0.7	0.6	0.5	0.4	0.1	0.1	0.1	0.1	0.0	0.6	0.0	0.0	0.1
PMV_{+W}	-0.8	0.5	-0.7	0.6	0.5	-0.3	0.1	0.1	0.0	0.0	0.1	0.0	0.6	0.0	0.2
PMV_{+S}	-0.8	0.5	-0.6	0.5	0.5	-0.5	0.1	0.1	0.0	0.0	0.7	0.0	0.0	0.0	0.1
PMV_{+E}	-0.8	0.5	-0.6	0.5	0.5	0.4	0.1	0.1	0.7	0.6	0.0	0.0	0.0	0.0	0.1
PMV_{+C}	-0.1	1.0	-0.1	0.4	0.1	0.0	0.7	0.6	0.1	0.1	0.0	0.0	0.1	-0.5	0.1

	U_{wS}	WWR_S	E_s	U_{wW}	U_{wE}	U_{wN}	D_{ohS}	D_{ohE}	D_{ohW}	T_{ifr}	D_{ohN}	L	WWR_N	WWR_W	T_{sh}
PMV_{+N}	0.0	0.0	0.0	0.0	0.0	-0.4	0.0	0.0	0.0	-0.2	-0.3	-0.1	0.2	0.0	0.0
PMV_{+W}	0.0	0.0	0.0	-0.5	0.0	0.0	0.0	-0.3	0.0	-0.2	0.0	0.0	0.0	0.1	0.0
PMV_{+S}	-0.5	0.5	0.0	0.0	0.0	0.0	-0.4	0.0	0.0	0.0	0.0	0.0	0.0	0.0	0.0
PMV_{+E}	0.0	0.0	0.0	0.0	-0.4	0.0	0.0	0.0	-0.4	0.0	0.0	0.0	0.0	0.0	0.0
PMV_{+C}	0.0	0.0	0.5	-0.1	0.0	0.0	0.0	-0.1	0.0	0.0	0.0	-0.2	0.1	0.0	0.0

I_{75pa}, the most influential design variable, has influence on the thermal comfort for the peripheral zones but not so much for the core zone as the infiltration occurs through the envelope, i.e. walls in contact with the exterior. Infiltrations can affect comfort because of the limited airflow rate, which means that the HVAC system is not always able to reach the desired set points depending on the combination of design variables. It is the opposite with T_{spc}, which is dominating in the core zone. As there is less heat loss in that zone, it is more often in a cooling mode than the peripheral zones. It is also interesting to note that the orientation of the building increases the comfort in some zones and at the same time decreases it in other zones. Finally, it is visible that variables related to a specific façade have much more impact on the comfort in the zone related to that façade than in the other zones. For example, $SHGC_E$ influences strongly PMV_+ in the east zone but not so much in the other zones.

5.5 Sobol second-order indices and interactions between variables

The first two techniques (SRC, PRCC) were suitable to give an appreciation of the most important variables. The second order Sobol indices S_{ij} can be used to identify interactions between 2 variables. They express the variance of an output caused by these binary interactions. When taken separately, the first order Sobol indices S_i of two variables do not represent the total variance introduced by these variables since it does not account for interactions. First-order indices S_i were calculated for all the outputs studied in this paper. It was found that the information available from these coefficients is essentially the same as what was revealed by the SRC and PRCC techniques, and therefore, it is not reproduced here. However, the second order Sobol indices were determined and are presented here.

In order to obtain valid results, the design sample needed to be larger than for the determination of SRC and PRCC. It was observed that with ~10,000 combinations of variables, the values of S_{ij} stabilized. Then, an evaluation second-order indices for all possible combinations of two variables was performed and the resulting indices are reported in Figs. 12 and 13. On the x and y-axes, each number represents a design variables which can be connected to the variables listed in Table 2. A high value (red color) means that the interaction is more important than a lower value (blue color).

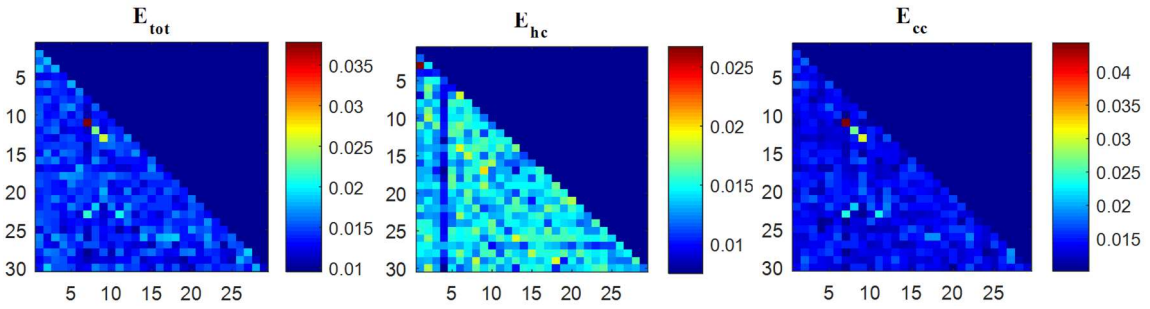

Figure 12: Second-order Sobol index S_{ij} for E_{tot}, E_{cc} and E_{hc}.

For E_{tot}, the most important interactions are related to the following pairs of variables: WWR_E - $SHGC_E$, WWR_S - $SHGC_S$ and WWR_W - $SHGC_w$. This makes sense as in the window heat balance, what really matters is actually the product of the window surface area and the SHGC of that specific window. As mentioned before, E_{cc} is the major contribution to E_{tot}, so one can notice the same dominant combinations of variables for E_{cc}

as for E_{tot}. The other combinations of variables for E_{tot} and E_{cc} were found to have a weak effect.

When looking at E_{hc}, it is interesting to observe a blue vertical line corresponding to the variable I_{75pa}. Although it is one of the most influential variables for E_{hc}, this variable is not significantly interacting with other variables. The main interactions occur for C_{ins} - T_{ins}, WWR_W - $U_{W\_W,}$ $SHGC_W$ - T_{sc}, WWR_N - U_{W_N}, WWR_N - WWR_E. The thickness of the insulation over its conductivity (T_{ins}/C_{ins}) actually corresponds to the thermal resistance of the opaque portion of the envelope, and it is this variable that truly influences thermal losses during winter rather than the two variables independently, which is why this interaction stands out for E_{hc}. The same analysis is valid for the pairs WWR - U_w. Although a larger window can increase solar gains, heat losses through fenestration are dictated by the product of U_w and of the window surface area and can become dominant over the solar gains during the heating mode, depending on the façade. Finally, regarding E_{hum} and E_{fan} (not shown in Fig. 12), there was no evidence of specific interactions.

The same analysis was done for the comfort criteria PMV_+ and the results are presented in Fig. 13. In general, for the four peripheral zones, the WWR of a given façade orientation (WWR_x where x represents the façade orientation) is interacting strongly with C_{ins}, $T_{ins,}$ I_{75Pa}, $SHGC_x$, U_{wx} and T_{spc} in the determination of the thermal comfort indices. The interactions of WWR_x with C_{ins}, T_{ins}, $SHGC_x$ and U_{wx} are due to the fact that together they influence the temperature of the internal surface of the envelope which has a strong effect on thermal comfort. Similarly, the combined effect of the surface temperature and air temperature (via T_{spc} and I_{75Pa}) affect the value of the operative temperature which is used to determine the level of thermal comfort. These interactions are harder to observe when looking at the general comfort index PMV_{+tot}. For PMV_{+C} and PMV_{+tot}, interactions were found to be weaker. The only interaction that was noticed is between T_{spc} and T_{spc}. Figure 11 shows that those two variables are among the most influents for PMV_{+C} and PMV_{+tot}. Figure 13 shows an interaction between them. In other words, the values of T_{spc} and T_{spc} should not be fixed independently in order to optimize thermal comfort.

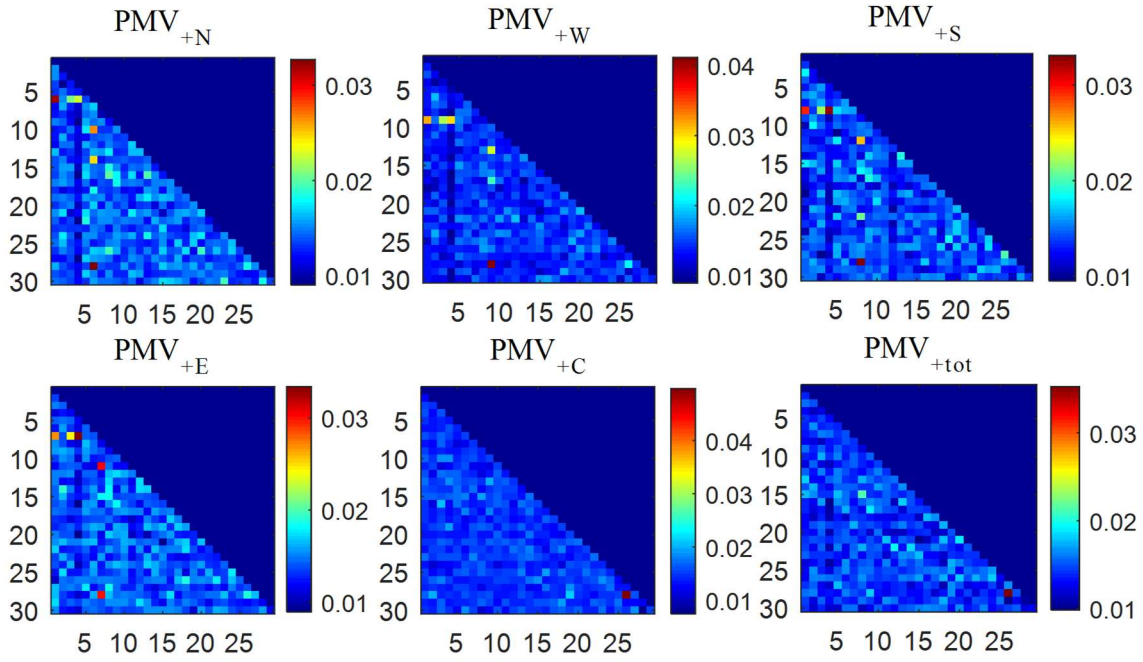

Figure 13: Second order Sobol index S_{ij} for PMV_{+} in each zone and $PMV_{+tot.}$

6 Sensitivity analysis versus phases of a design process

In Section 5, three techniques of SA have been applied in order to find which of the design variables were the most influential depending on the output functions considered. Although this analysis revealed dominating variables and interactions of variables, it does not consider the different and sequential phases of a real design process during which a limited number of variables are chosen at a time.

In a traditional design process (TDP), the values of given variables presented in Table 2 are fixed or chosen sequentially during specific phases of the project by the appropriate specialists. However, there is an emerging trend to design with a multi-disciplinary team from the early stage of the design process [66]. In the integrated design process (IDP), all specialists are teamed up in the design process allowing to avoid the sequential phases and irreversible choices inherent to the TDP. This approach is believed to help achieving more sustainable building designs [4], [5].

To some extent, one can suppose that all design variables can be included together in the analysis if an “extreme” IDP was considered. This corresponds to the results presented in Section 5 in which all 30 design variables were included at the same time in the SA.

However, in a TDP, it is worth to study the impact of the sequential design phases on the results of the SA. Note that in a complete building design process, several other objectives have to be looked at, apart from energy and thermal comfort (e.g., structure, GHG emissions, etc.). However, this was not explored in the present work and only the impact of the design process on these above-mentioned performance criteria was studied. Furthermore, it is worth to mention that the design process itself was not included as a design variable in Table 2 since only continuous variables were used, and this would have been a discrete variable. Instead, the following methodology was developed to investigate the impact of the design process.

In this paper, the TDP is represented by the framework developed by [67] and shown in Fig. 14. The involvement of the different professionals during the different phases of a TDP is shown on a timeline, from P0 (pre-design) to P5 (building operation). As the work of stakeholders can be related to choosing values for specific design variables, these variables are also represented on the timeline. It should be noted that this classification should not be considered as "absolute" but rather as a general representation of the TDP in order to evaluate the potential impact of the design phases on the SA results.

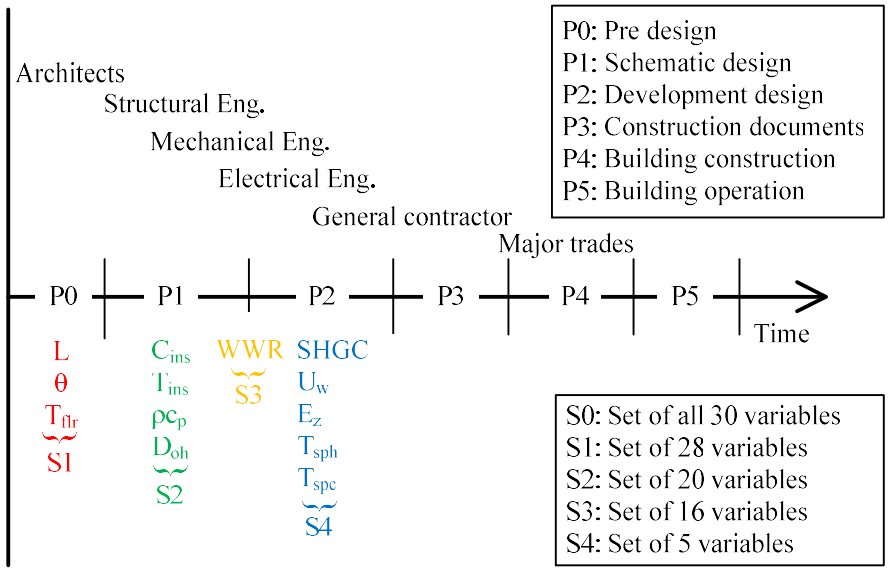

Figure 14: Timeline representing the typical phases of a TDP.

The design variables have been separated along the phases between those that are already fixed from previous phases, those to be chosen at that particular phase, and those that will

be determined later. The set of variables S0 contains all the 30 variables introduced earlier. S1 is the set of design variables, except L and θ which are determined in phase P0. A similar approach was used at each phase as shown in Fig. 14, with the sets of variables S1, S2, S3 and S4 containing respectively the 30 variables minus the ones chosen at the previous phases. For each one of these sets of variables (i.e., S0 to S4), a new SA on the energy and comfort criteria was performed by fixing the variables not included in the sets (these variables were fixed to the closest values that were actually chosen by designers in the reference building introduced in Section 2). In other words, the SA is performed from the standpoint of a designer during the TDP for which some variables are already fixed and unchangeable. Since the number of design variables is reduced after each phase, the chosen size of the sample was also changed during each successive SA (from 2,000 to 600).

6.1 General results from the energy consumption and comfort distributions

Table 5 shows the average, standard deviation and y values of the output functions E_{tot} and PMV_{+tot} according to a specific set of variables (y is determined from Eq. (8) One can notice that when looking at the distribution of energy consumption over all the simulated combinations, there are many possibilities to find a high performance design during the early phase (i.e. when no variable is fixed at S0) but as one fixes variables, those possibilities are reduced.

Table 5: Average, standard deviation and y values of E_{tot} and PMV_{+tot} for each set of variables (as defined in Fig. 14).

		S0	S1	S2	S3	S4
E_{tot} [kWh/m^2]	$\bar{x}$	78	78	84	101	90
	σ	10.8	11.3	13.2	11.2	5.4
	y	0.85	0.87	0.93	1.00	1.00
PMV_{+tot} [hr]	$\bar{x}$	2415	2395	2311	2408	1875
	σ	187	197	178	142	146
	y	0.85	0.85	0.86	0.88	0.98

For the first set (S0), the average energy consumption was 78 kWh/m^2 with a standard deviation of 10.8 kWh/m^2 and in the last set (S4), these values become 90 and 5.4 kWh/m^2 respectively. For PMV_{+tot}, one finds that during the last phase, on average, there are more scenarios where the comfort is better compared to S1. It is important to recall that the

results of Table 5 depend of the values chosen for the fixed variables. In this particular case, after S3, the values of the remaining design variables were well selected in order to achieve a comfortable design.

To observe the influence of fixing variables on the SA results, the β_i coefficients were also calculated for E_{tot} and PMV_{+tot} after each phase. The SRC approach was adopted based on the analysis presented in Section 4 and the evaluation of Section 5.1. A first observation from Table 5 is that after fixing variables, the system becomes more and more linear (y values from Eq. (8) tend to 1). There are also several interactions between the variables as it was presented in Section 5.5 However, when the SA is performed with the set S4, the inputs variation explains 100% of the variation of E_{tot} and 98% of the variation of PMV_{+tot}. Fixing a variable in one phase that has interactions with variables in another phase means that the designer cannot take advantage of the interactions anymore.

6.2 Results from sensitivity analysis with respect to E_{tot}

For a better understanding of the consequences of fixing variables along the design phases, Fig. 15 presents the evolution of the β_i values with respect to E_{tot}. One can observe that the first two phases of the design process are focussed on selecting variables that are not very influential ($\beta_i < 0.1$) in terms of energy consumption (i.e., L, θ and T_{flr} for S0, and D_{oh}, T_{ins}, C_{ins} and ρc_p for S1). In this specific situation, it does not affect the probability to find "optimal" solutions as can be seen in Table 5 when looking at the evolution of $\bar{x}$ and σ between S0 and S1.

However, in the following design steps (S2, S3 and S4), variables among the most influential in terms of energy consumption are selected. For example, WWRs have high β-values (from 0.16 to 0.53 depending on the façade) at step S3. When the WWRs are fixed in that step, WWRs of 55%, 36%, 34% and 40% were assigned for the north, east, south and west façades respectively, corresponding to the values of the reference building. This had the effect of increasing the average of E_{tot} from 84 to 101 kWh/m^2 between S2 and S3. In other words, the choice of WWRs limited the design space to less energy performant designs in that case.

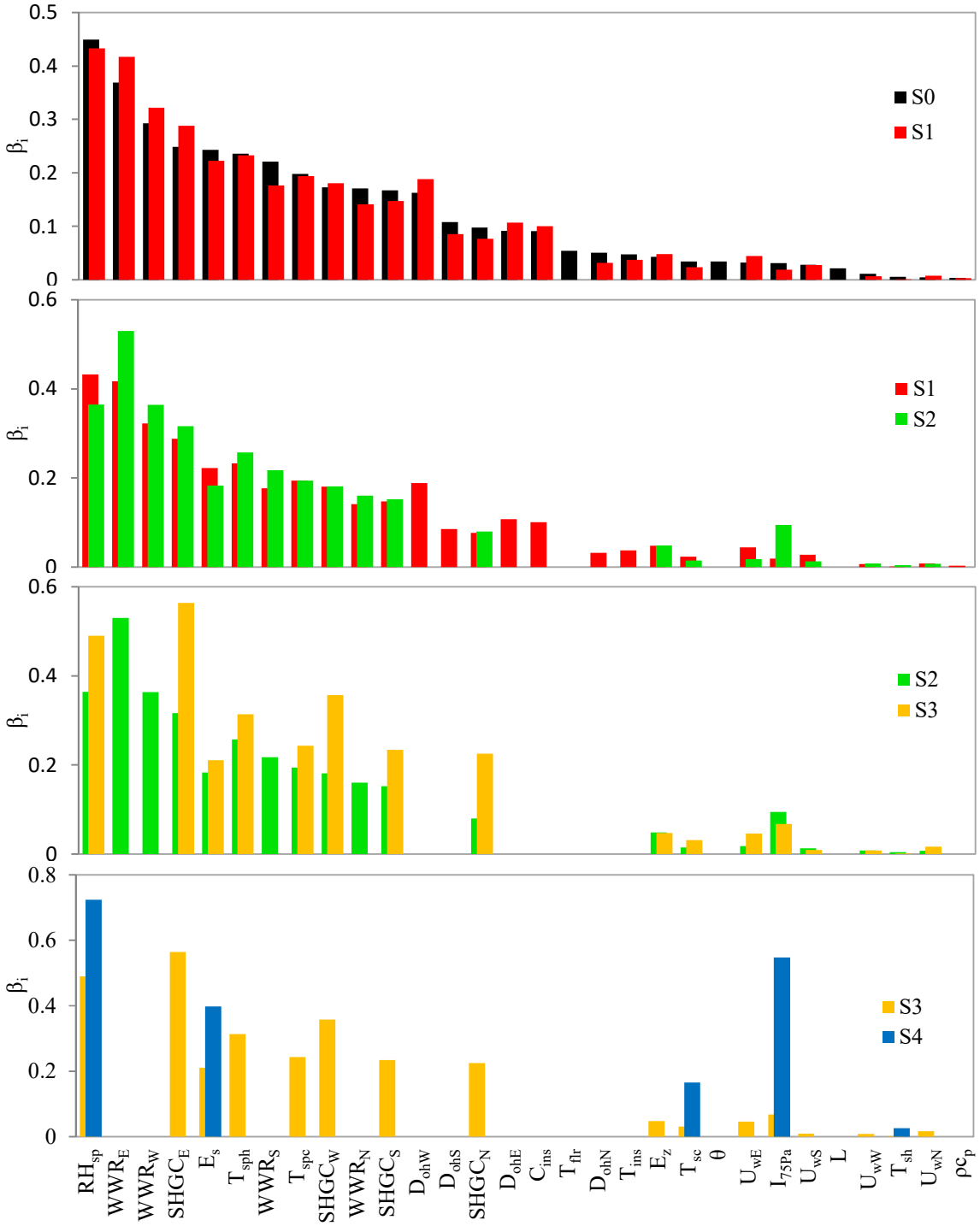

Figure 15: Absolute β_i-values before and after fixing variables during the design process for E_{tot}.

Another important observation from Fig. 15 is that throughout the design process, some variables may gain or lose importance (i.e. their ranking and/or β_i-values can change). For example, once the aspect ratio, the orientation of the building and the height of the floor

have been fixed in S0, the variables WWR_S and WWR_N are losing importance regarding E_{tot} whereas WWR_E and WWR_W become more influential. This can be an indication that L, θ and WWR are interacting all together and that it could be advantageous to consider them at the same time to achieve an optimized design in term of energy consumption. If we look back at the details of Fig. 12, similar conclusions were expressed by S_{ij}-values. The four strongest interactions observed with the length of the building are related to WWR_N, WWR_W, θ and T_{flr}.

Moreover, one can notice in Fig. 15 the sudden growth of importance of the SHGCs after fixing the WWRs. As mentioned before, the cooling energy is dominant in this case. When the WWRs are not fixed, the values of SHGCs are not so important for the energy balance. However, when fixed, the SHGCs are the most important remaining variables that can strongly influence the solar heat gain. In that specific case, D_{oh} was fixed before SHGCs to a value of 0 m, which means that there are no solar overhangs.

Finally, one more conclusion can be drawn from the sudden increase of the SRC for I_{75Pa} in S4. When almost all variables have been fixed, it becomes important to control this variable. However, it is known that I_{75Pa} depends on many other design decisions, e.g. the composition of the envelope, the choice of windows, the ventilation strategy, the construction quality and more. In other words, in practice the value of this variable can be evaluated at the end of a design process but should be considered during the early phases.

6.3 Results from sensitivity analysis with respect to PMV_{+tot}

The same analysis was performed with PMV_{+tot} and the results are presented in Fig. 16. It is visible that the first two sets of variables are not among the most important in terms of PMV_{+tot}. Furthermore, the β-values of the design variables with respect to PMV_{+tot} are sometimes changing more significantly during the design process compared to E_{tot}. For example, the WWRs become very important in S2 although some of them were irrelevant in the initial set (e.g., β of WWR_N and WWR_W almost equal to zero in S0). When one sums the β coefficients of WWRs, the result is 0.19 for the set S0 and 0.58 for S2. In other words, only 18% of the variance of the PVM was explained by these variables in S0 whereas 58% of the variance is explained by them in S2. It should be recalled that in S2, L, θ, T_{flr}, D_{oh},

T_{ins}, C_{ins} and ρc_p were fixed. In S1, the variance of T_{ins} and C_{ins} was accounting for about 50% of the variance of the comfort, which means that these two variables are important for the summer comfort. A better insulation will reduce E_{hc} but will increase PMV_{+tot}.

In the last set of variables (S4), T_{sc} becomes the most important variable in front of RH_{sp} and I_{75Pa}. From S0 to S3, the β-value of T_{sc} remains stable around 0.13 and in phase S4, the value increased to 0.82. After fixing most of the variables, T_{sc} becomes one of the only unfixed variables that will affect comfort. In this building, the rooms are often too warm and the dominating energy demand comes from the cooling coil. As a result, natural ventilation strategies or infiltration rate, the shading strategies, the composition of the envelope and T_{sc} should be considered at the same time in order to select performant designs.

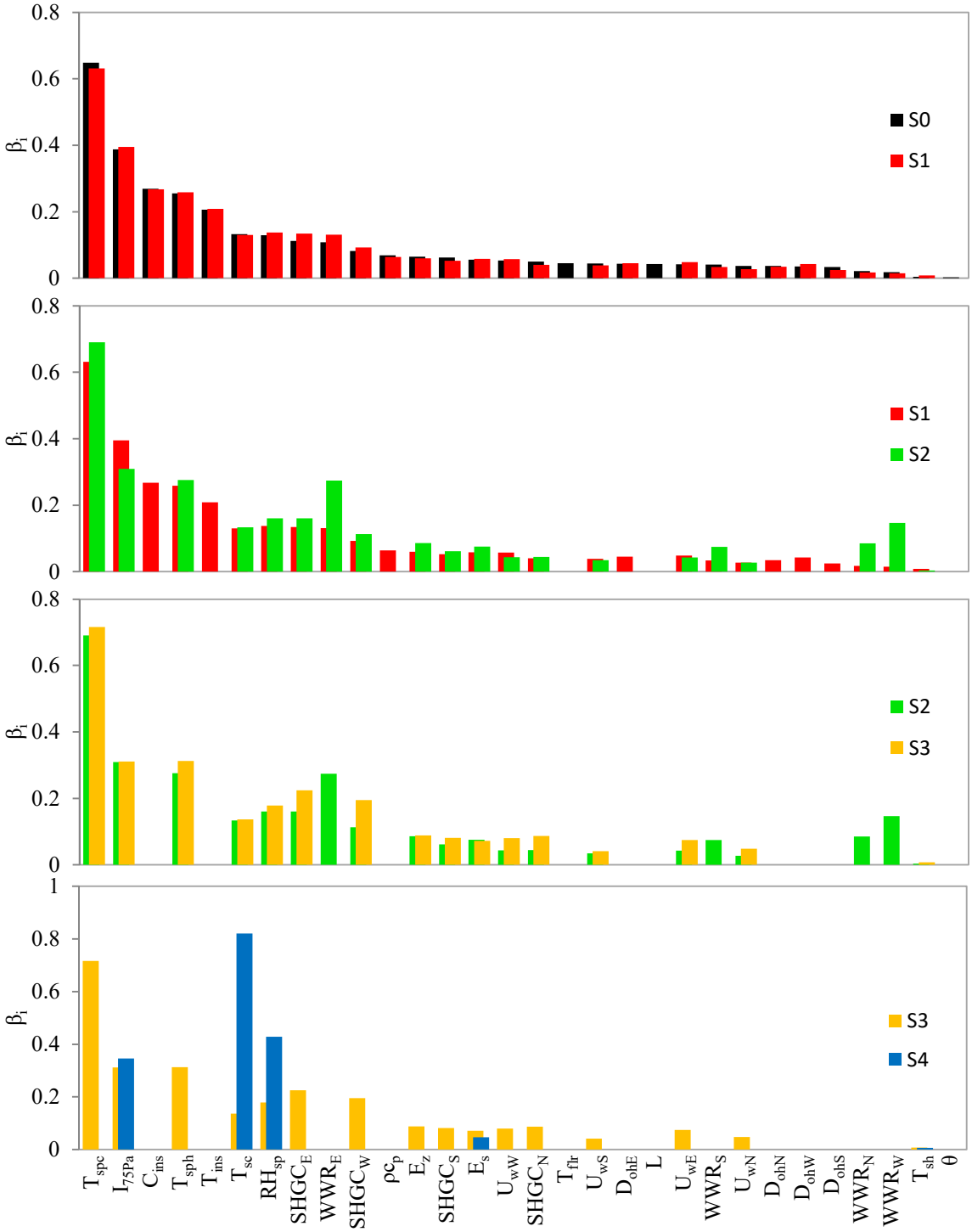

Figure 16: Absolute β_i-values before and after fixing variables during the design process for PMV_{+tot}.

7 Conclusions

This paper uses SA techniques in order to evaluate how 30 design variables affect building performance related to energy and comfort. At first, an SRC analysis showed that about half of the variables do not have impact on the annual energy consumption (E_{tot}). However, looking at the details of where energy is consumed (e.g. energy of cooling or heating coil, i.e. E_{cc}, E_{hc}) led to a different story. For example, the infiltration rate is irrelevant for E_{tot} but the most influential parameter for E_{hc}. Increasing the value of this variable increases E_{hc} but reduces E_{cc}. The same observations apply to the thickness and thermal conductivity of insulation material.

Additionally, according to the simulation results, it was rarely too cold (low PMV) and often too warm (high PMV) in the building in the different scenarios tested over the course of the sensitivity analysis. The PRCC technique has been applied to several comfort model outputs and only a few parameters were found to affect significantly the average comfort. Among them are the infiltration rate, temperature set points, and thickness and thermal conductivity of the insulation material. However, some variables had different importance and in some cases even an opposite effect on the comfort in different zones of the building.

In a third step, Sobol second order index were used to observe the interactions between variables. This technique was successful to detect several interactions. Among them, the WWR-SHGC pairs were the most visible.

A methodology was then proposed to study the evolution of the influence of the design variables throughout a traditional design phase in which variables are chosen sequentially. The variables were grouped in 5 sets that were fixed sequentially, before performing a sensitivity analysis with the remaining “free” variables. This framework demonstrated that the TDP could reduce the opportunities to find optimal solutions with respect to annual energy consumption. In fact, variables with a small influence on the energy consumption were fixed in the first two phases of the TDP. When influential variables began to be chosen in the third step, namely the WWRs, changes in the ranking of importance of the remaining variables were observed. This comparison between IDP and TDP shows the importance of the design process on the final building performance and quantify the interest of using a holistic design approach.

In addition to providing an appreciation of the most influential variables and interactions for the present reference building, this paper illustrates how the building design process can change the relevance of some design variables and ultimately, the performance of the building. Including more design variables simultaneously in the early stages of the design process can help to achieve more sustainable buildings, with tools such as SA techniques and multi-objective optimization strategies. Future work could focus on including other important objectives that were not considered in the present study, such as aesthetics, structural capacity, vibrations, resistance to fire and earthquake, visual comfort, carbon emissions, etc., as well as other design variables.

8 Acknowledgements

This work was supported by the Industrial Research Chair on Eco-Responsible Construction (CIRCERB) and by the Natural Sciences and Engineering Research Council of Canada (NSERC).

9 References

[1] E. and C. C. C. Government of Canada, "Environmental Indicators - Greenhouse Gas Emissions by Economic Sector," 16-Mar-2012. [Online]. Available: https://www.ec.gc.ca/indicateurs-indicators/default.asp?lang=en&n=F60DB708-1. [Accessed: 01-Jan-2017].

[2] Government of Canada, "Energy," 01-Jan-2017. [Online]. Available: http://www.statcan.gc.ca/pub/11-402-x/2012000/chap/ener/ener-eng.htm. [Accessed: 01-Jan-2017].

[3] UNEP SBCI, "Buildings and Climate Change," 2009.

[4] R. Azari and Y.-W. Kim, "Evaluating integrated design process of High-Performance green buildings," Seattle, WA, 2013.

[5] B. Poel, "Integrated design with a focus on energy aspects," *ECEEE 2005 Summer Study*, vol. 9, pp. 109–120, 2005.

[6] M. Abaza, "High Performance Buildings using Whole Building Integrated Design Approach," *ASHRAE Trans.*, vol. 117, no. 1, pp. 240–247, 2011.

[7] R. Azari and Y.-W. Kim, "Integration Evaluation Framework for Integrated Design Teams of Green Buildings: Development and Validation," *J. Manag. Eng.*, vol. 32, no. 3, pp. 1–14, May 2016.

[8] R. Azari and Y.-W. Kim, "Development and Validation of a Framework for Evaluation of Integrated Design Teams of Sustainable High-Performance Buildings," in *Construction Research Congress 2014: Construction in a Global Network*, 2014, pp. 584–593.

[9] S. Mollaoglu-Korkmaz, L. Swarup, and D. Riley, "Delivering sustainable, high-performance buildings: Influence of project delivery methods on integration and project outcomes," *J. Manag. Eng.*, vol. 29, no. 1, pp. 71–78, 2011.
[10] S. Korkmaz, D. Riley, and M. Horman, "Piloting Evaluation Metrics for Sustainable High-Performance Building Project Delivery," *J. Manag. Eng.*, vol. 136, no. 8, pp. 877–885, 2010.
[11] D. Garcia Sanchez, B. Lacarrière, M. Musy, and B. Bourges, "Application of sensitivity analysis in building energy simulations: Combining first- and second-order elementary effects methods," *Energy Build.*, vol. 68, pp. 741–750, Jan. 2014.
[12] P. Heiselberg, H. Brohus, A. Hesselholt, H. Rasmussen, E. Seinre, and S. Thomas, "Application of sensitivity analysis in design of sustainable buildings," *Renew. Energy*, vol. 34, no. 9, pp. 2030–2036, Sep. 2009.
[13] J. Yu, L. Tian, C. Yang, X. Xu, and J. Wang, "Sensitivity analysis of energy performance for high-rise residential envelope in hot summer and cold winter zone of China," *Energy Build.*, vol. 64, pp. 264–274, Sep. 2013.
[14] B. Eisenhower, Z. O'Neill, S. Narayanan, V. A. Fonoberov, and I. Mezić, "A methodology for meta-model based optimization in building energy models," *Energy Build.*, vol. 47, pp. 292–301, Apr. 2012.
[15] A. P. Ramallo-González and D. A. Coley, "Using self-adaptive optimisation methods to perform sequential optimisation for low-energy building design," *Energy Build.*, vol. 81, pp. 18–29, Oct. 2014.
[16] Trane Canada, "4905 Immeuble Lapinière Complexe LL : Manuel d'instruction complet avec plans de contrôle." 2010.
[17] J. D. Spitler, *Load Calculation Applications Manual (I-P Edition)*, 2nd Edition. Atlanta, GA: ASHRAE, 2009.
[18] *BS EN ISO 7730:1995 Moderate thermal environments – Determination of the PMV and PPD indices and specification of the conditions for thermal comfort*. British Standards Institution, 2005.
[19] American Society of Heating Refrigerating and Air-Conditioning Engineers, *ASHRAE standard 62.1 : Ventilation for Acceptable Indoor Air Quality*. Atlanta, GA: ASHRAE, 2001.
[20] Trane, "Indoor Air Quality, a guide to understanding ASHRAE standard 62-2001." American Standard Inc., 2002.
[21] D. Larin, "Complex L.L. Phase II 4905 Lapinière : Ventilation étage type." Blondin Fortin, 2009.
[22] A. A. Bell, *HVAC: equations, data, and rules of thumb*. New York: McGraw-Hill, 2000.
[23] "TRNSYS 17 - Volume 5 Multizone building modeling with Type56 and TRNBuild." Solar Energy Laboratory, 2012.
[24] American Society of Heating Refrigerating and Air-Conditioning Engineers, *ANSI/ ASHRAE Standard 55 (2004): Thermal Comfort Conditions for Human Occupancy*. Atlanta, GA: ASHRAE, 2004.
[25] M. De Carli, B. W. Olesen, A. Zarrella, and R. Zecchin, "People's clothing behaviour according to external weather and indoor environment," *Build. Environ.*, vol. 42, no. 12, pp. 3965–3973, Dec. 2007.

[26] E. Asadi, M. G. da Silva, C. H. Antunes, and L. Dias, "A multi-objective optimization model for building retrofit strategies using TRNSYS simulations, GenOpt and MATLAB," *Build. Environ.*, vol. 56, pp. 370–378, Oct. 2012.
[27] Natural Resources Canada, "EE4," 08-Jan-2009. [Online]. Available: https://www.nrcan.gc.ca/energy/software-tools/7453. [Accessed: 18-Oct-2017].
[28] Gourvernement du Québec, "Politique Énergétique : L'énergie des québécois, source de croissance," Gourvernement du Québec, 2016.
[29] C. Turner and M. Frankel, "Energy performance of LEED for New Construction Buildings," 2008.
[30] L. Magnier and F. Haghighat, "Multiobjective optimization of building design using TRNSYS simulations, genetic algorithm, and Artificial Neural Network," *Build. Environ.*, vol. 45, no. 3, pp. 739–746, Mar. 2010.
[31] Y. Bichiou and M. Krarti, "Optimization of envelope and HVAC systems selection for residential buildings," *Energy Build.*, vol. 43, no. 12, pp. 3373–3382, Dec. 2011.
[32] W. Wang, R. Zmeureanu, and H. Rivard, "Applying multi-objective genetic algorithms in green building design optimization," *Build. Environ.*, vol. 40, no. 11, pp. 1512–1525, Nov. 2005.
[33] M.-C. Hamelin and R. Zmeureanu, "Multi-objective life cycle optimization of a single-family house envelope," presented at the The Canadian Conference on Building Simulation, Halifax, NS, 2012, pp. 202–214.
[34] S. Bucking, "Multi-Objective Optimal Design of a Near Net Zero Energy Solar House," *ASHRAE Trans.*, vol. 120, pp. 224–235, 2014.
[35] M. Hamdy, A. Hasan, and K. Siren, "Impact of adaptive thermal comfort criteria on building energy use and cooling equipment size using a multi-objective optimization scheme," *Energy Build.*, vol. 43, no. 9, pp. 2055–2067, Sep. 2011.
[36] D. Gossard, B. Lartigue, and F. Thellier, "Multi-objective optimization of a building envelope for thermal performance using genetic algorithms and artificial neural network," *Energy Build.*, vol. 67, pp. 253–260, Dec. 2013.
[37] M. Hamdy, A. Hasan, and K. Siren, "Applying a multi-objective optimization approach for Design of low-emission cost-effective dwellings," *Build. Environ.*, vol. 46, no. 1, pp. 109–123, Jan. 2011.
[38] M. Ferrara, E. Fabrizio, J. Virgone, and M. Filippi, "A simulation-based optimization method for cost-optimal analysis of nearly Zero Energy Buildings," *Energy Build.*, vol. 84, pp. 442–457, Dec. 2014.
[39] Y. Lu, S. Wang, Y. Zhao, and C. Yan, "Renewable energy system optimization of low/zero energy buildings using single-objective and multi-objective optimization methods," *Energy Build.*, vol. 89, pp. 61–75, Feb. 2015.
[40] S. Schiavoni, F. D'Alessandro, F. Bianchi, and F. Asdrubali, "Insulation materials for the building sector: A review and comparative analysis," *Renew. Sustain. Energy Rev.*, vol. 62, pp. 988–1011, Sep. 2016.
[41] H. Omrany, A. Ghaffarianhoseini, A. Ghaffarianhoseini, K. Raahemifar, and J. Tookey, "Application of passive wall systems for improving the energy efficiency in buildings: A comprehensive review," *Renew. Sustain. Energy Rev.*, vol. 62, pp. 1252–1269, Sep. 2016.

[42] Z. Lianying, W. Yuan, Z. Jiyuan, L. Xing, and Z. Linhua, "Numerical Study of Effects of Wall's Insulation Thickness on Energy Performance for Different Climatic Regions of China," *Energy Procedia*, vol. 75, pp. 1290–1298, Aug. 2015.
[43] K. Gowri, D. Winiarski, and R. Jarnagin, "Infiltration modeling guidelines for commercial building energy analysis," *Pac. Northwest Natl. Lab.*, 2009.
[44] American Society of Heating Refrigerating and Air-Conditioning Engineers, Inc., *ASHRAE Handbook - Fundamentals (SI Edition)*. Atlanta, GA: ASHRAE, 2013.
[45] American Society of Heating Refrigerating and Air-Conditioning Engineers, *ANSI/ASHRAE Standard 90.1 (2010): Energy Standard for Buildings Except Low-Rise Residential Buildings*. Atlanta, GA: ASHRAE, 2010.
[46] L. Gosselin and J.-M. Dussault, "Correlations for glazing properties and representation of glazing types with continuous variables for daylight and energy simulations," *Sol. Energy*, vol. 141, pp. 159–165, 2017.
[47] S. B. Sadineni, S. Madala, and R. F. Boehm, "Passive building energy savings: A review of building envelope components," *Renew. Sustain. Energy Rev.*, vol. 15, no. 8, pp. 3617–3631, Oct. 2011.
[48] R. Charron and A. Athienitis, "The use of genetic algorithms for a net-zero energy solar home design optimisation tool," in *Proceedings of PLEA 2006 (Conference on Passive and Low Energy Architecture), Geneva, Switzerland*, 2006.
[49] A. Alajmi and J. Wright, "Selecting the most efficient genetic algorithm sets in solving unconstrained building optimization problem," *Int. J. Sustain. Built Environ.*, vol. 3, no. 1, pp. 18–26, Jun. 2014.
[50] M. Hamdy, A. Hasan, and K. Siren, "A multi-stage optimization method for cost-optimal and nearly-zero-energy building solutions in line with the EPBD-recast 2010," *Energy Build.*, vol. 56, pp. 189–203, Jan. 2013.
[51] D. O'Connor, J. K. S. Calautit, and B. R. Hughes, "A review of heat recovery technology for passive ventilation applications," *Renew. Sustain. Energy Rev.*, vol. 54, pp. 1481–1493, Feb. 2016.
[52] P. M. Cuce and S. Riffat, "A comprehensive review of heat recovery systems for building applications," *Renew. Sustain. Energy Rev.*, vol. 47, pp. 665–682, Jul. 2015.
[53] A. Mardiana-Idayu and S. B. Riffat, "Review on heat recovery technologies for building applications," *Renew. Sustain. Energy Rev.*, vol. 16, no. 2, pp. 1241–1255, Feb. 2012.
[54] D. Stanke, "System operation: dynamic reset options," *ASHRAE J.*, vol. 48, no. 12, pp. 18–32, 2006.
[55] D. Int-Hout, "Overhead Heating : Revisiting a Lost Art," *ASHRAE J.*, vol. 49, no. 3, pp. 56–63, 2007.
[56] G. Wang and L. Song, "Air handling unit supply air temperature optimal control during economizer cycles," *Energy Build.*, vol. 49, pp. 310–316, Jun. 2012.
[57] CMHC, "Moisture and air: A guide for understanding and fixing interior moisture problems in housing." Canada Mortgag and Housing Corporation, 2015.
[58] S. J. Emmerich and A. K. Persily, "US commercial building airtightness requirements and measurements," in *AIVC Conference*, 2011.
[59] A. Saltelli, Ed., *Global sensitivity analysis: the primer*. Chichester, England ; Hoboken, NJ: John Wiley, 2008.

[60] W. Tian, “A review of sensitivity analysis methods in building energy analysis,” *Renew. Sustain. Energy Rev.*, vol. 20, pp. 411–419, Apr. 2013.
[61] A.-T. Nguyen and S. Reiter, “A performance comparison of sensitivity analysis methods for building energy models,” *Build. Simul.*, vol. 8, no. 6, pp. 651–664, Dec. 2015.
[62] F. Grégoire, L. Gosselin, and H. Alamdari, “Sensitivity of Carbon Anode Baking Model Outputs to Kinetic Parameters Describing Pitch Pyrolysis,” *Ind. Eng. Chem. Res.*, vol. 52, no. 12, pp. 4465–4474, Mar. 2013.
[63] A. Saltelli and I. M. Sobol’, “About the use of rank transformation in sensitivity analysis of model output,” *Reliab. Eng. Syst. Saf.*, vol. 50, no. 3, pp. 225–239, 1995.
[64] B. Durand-Estebe, J. Lopez, and L. Mora, “Intégration et tests de méthodes d’analyse de sensibilité et de propagation d’incertitudes appliquées à la simulation thermique dynamique de bâtiment,” presented at the Conférence IBPSA France, Marne la Vallée, France, 2016, p. 8.
[65] E. Plischke, “An effective algorithm for computing global sensitivity indices (EASI),” *Reliab. Eng. Syst. Saf.*, vol. 95, no. 4, pp. 354–360, Apr. 2010.
[66] B. Metz and Intergovernmental Panel on Climate Change, Eds., *Climate change 2007: mitigation of climate change: contribution of Working Group III to the Fourth assessment report of the Intergovernmental Panel on Climate Change*. Cambridge ; New York: Cambridge University Press, 2007.
[67] Busby Perkins+Will and Stantec consulting, “Roadmap for the integrated design process,” BC Green Building Roundtable, Vancouver, 2007.